

## Water-solid triboelectric nanogenerators: An alternative means for harvesting hydropower



Dongyue Jiang<sup>a,\*</sup>, Minyi Xu<sup>b</sup>, Ming Dong<sup>a</sup>, Fei Guo<sup>a</sup>, Xiaohua Liu<sup>a</sup>, Guijun Chen<sup>a</sup>,  
Zhong Lin Wang<sup>c,d,\*\*</sup>

<sup>a</sup> Key Laboratory of Ocean Energy Utilization and Energy Conservation of Ministry of Education, Dalian University of Technology, Liaoning Province, 116024, China

<sup>b</sup> Marine Engineering College, Dalian Maritime University, Liaoning Province, 116026, China

<sup>c</sup> Beijing Institute of Nanoenergy and Nanosystems, Chinese Academy of Sciences, Beijing, 100083, China

<sup>d</sup> School of Materials Science and Engineering, Georgia Institute of Technology, Atlanta, GA, 30332, USA

### ARTICLE INFO

#### Keywords:

Hydropower  
Triboelectric nanogenerators  
Water-solid interface  
Energy harvesting  
Self-powered sensors  
Wave energy

### ABSTRACT

Hydropower is an important renewable resource, and is derived from the energy of falling, fast-running, and/or oscillating motions of water, including rainfall, tidal currents, waves, and river flows. Over the centuries, the kinetic energy of hydropower has generally been harvested for either replacing labour directly, or for generating power with electromagnetic generators (EMG). However, it is possible to ignore another important energy source contained in water: the triboelectric energy. Following the first report of water-solid triboelectric nanogenerators (TENG), several types of interesting systems have been studied for harvesting the hydropower from rainfall, tides, waves, river flows, etc. TENG devices provide power differently from EMGs; EMGs generate electricity by a Lorenz force-driven electron flow, whereas TENG devices produce power by asymmetric screening of triboelectric charges in the form of displacement current. With this mechanism, power generation is achieved using water contact and separation motions with the TENG devices. In addition, the output performance of a water-solid TENG device is different from that of EMGs in terms of current, voltage, and frequency. The present study comprehensively reviews water-solid TENG devices for hydropower harvesting. This review first addresses the formation of tribo-charges on a solid surface, followed by the configuration, working principles, and parameters affecting the output performance, as well as applications for energy harvesting and self-powered sensors and actuators. Finally, this study provides an outlook of potential opportunities and challenges.

### 1. Introduction

Hydropower originates from falling, fast-running, and/or oscillating motions of water. These types of moving water contain large amounts of mechanical energy. The utilisation of hydropower can be traced back to the 4th century BCE, for irrigation and replacing labour in the form of devices such as trip hammers and water mills [1]. In the first operation of a hydroelectric plant in Wisconsin in 1882, the electricity was generated by running water, and demonstrated a capacity of 12.5 kW [2]. Even in recent years, hydropower has remained a popular renewable energy source. In 2015, 16.6% of the total electricity was generated by hydropower worldwide, i.e. 70% of all of the renewable energy-produced electricity [3]. This is because hydroelectric plants consume fewer fossil fuels, and produce less greenhouse gases. In modern hydroelectric plants, a high-speed water flow is required for

electromagnetic generators (EMGs) to generate electricity, whereby the generated power can be integrated to a power network. However, a river flow speed is typically slow (0–3 m/s) [4], and does not meet the requirements for network integration. To increase the speed of the water flow, dams are typically constructed to increase the potential energy of the flowing water. The construction of dams not only increases the investment, but also brings adverse effects to social and ecological systems [5]. These factors limit the widespread utilisation of hydropower.

With the recent rapid development of micro/nano fabrication techniques, different types of nanogenerators have been proposed for harvesting mechanical energy [6–8]. A triboelectric nanogenerator (TENG) is a typical device for converting diverse types of mechanical energy into electricity, including human motion, vibration, wind, and flowing water [9]. EMGs generate electricity by a Lorenz force-induced

\* Corresponding author.

\*\* Corresponding author. Beijing Institute of Nanoenergy and Nanosystems, Chinese Academy of Sciences, Beijing, 100083, China.

E-mail addresses: [jiangdy@dlut.edu.cn](mailto:jiangdy@dlut.edu.cn) (D. Jiang), [zhong.wang@mse.gatech.edu](mailto:zhong.wang@mse.gatech.edu) (Z.L. Wang).

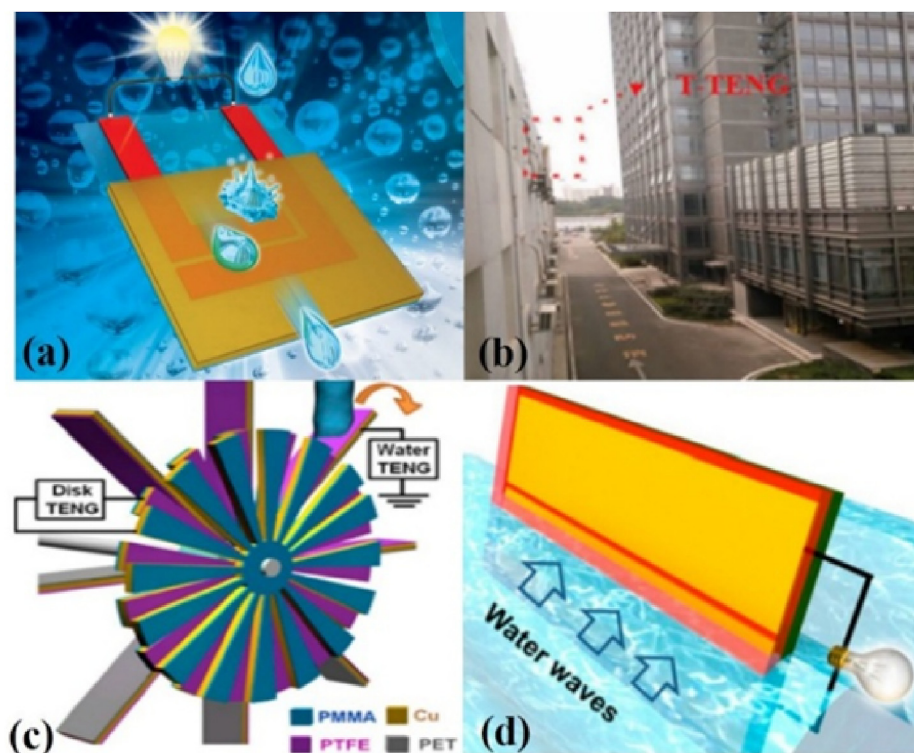


Fig. 1. Types of water-triboelectric nanogenerator (TENG) devices for harvesting hydropower from (a–b) raindrops, reproduced with permissions [15,16], Copyright 2014, Royal Society of Chemistry, Copyright 2015, Springer Nature Publishing AG, (c) water stream, reproduced with permissions [17], Copyright 2014, American Chemical Society, (d) water wave, reproduced with permissions [18], Copyright 2014, American Chemical Society.

electron flow when a conductor encircles a varying magnetic flux, whereas a TENG device outputs a displacement current driven by a triboelectric potential [10]. The power generation in a TENG device is achieved by a conjunction of the triboelectrification effect and electrostatic induction. When a mechanical motion is applied to a TENG device, contact is established between two thin organic/inorganic films of the TENG device exhibiting opposite tribo-polarities [11]. Such contact builds up a triboelectric potential between the two thin films. Upon separating the two thin films, the built triboelectric potential drives an electron flow through the external circuit, and generates electricity. Following the first report of a TENG device by Prof. Zhong Lin Wang's group at the Georgia Institute of Technology in 2012 [12], the power density and total efficiency have reached up to  $500 \text{ W/m}^2$  [13] and 85% [14], respectively. The triboelectric potential can also be realised via contact and separation motions between water and a solid surface. As compared to conventional EMGs, which require high-speed rotation, a water-TENG device can generate electricity in much simpler ways, including via droplets, tides, waves, and water streams interacting with the water-TENG devices. Fig. 1 presents schematics for harvesting the various types of aforementioned hydropower by water-TENG devices. In Fig. 1a, the TENG device harvests energy from raindrops; when a  $30 \mu\text{L}$  droplet impacts the water-TENG, the generated electricity can light up a LED light bulb [15]. In Fig. 1b, the concept of the raindrop energy harvesting is fabricated with a transparent feature, and is applied to the window of a building [16]. In Fig. 1c, the hydropower from a water stream is harvested by a water wheel-type TENG device [17]. In Fig. 1d, water wave motion from an arbitrary direction is harvested by a water-TENG device [18]. It can be seen that TENG devices are capable of harvesting diverse types of hydropower existing in nature, with high-power outputs. The recent research progress on liquid-solid based triboelectric energy harvesters was reviewed in Ref. [19]. However, the explanations regarding the formation of tribo-charges and the parameters affecting the output performance of water-TENG devices are inadequate. Therefore, this review investigates the research progress regarding the formation of tribo-charges, and the water-TENG working mechanisms, working modes, parameters, and applications in harvesting hydropower, as well as self-powered sensors/

actuators. Based on the progress in water-TENG devices, an outlook is provided to explain the challenges and opportunities in deploying water-TENG devices.

## 2. Working principle

When water is in contact with a solid surface, tribo-charges appear on the solid surface. The tribo-charges on the solid surface screen the electrons on the back electrodes. A current flow will be generated if a load is connected between the back electrode and ground, to balance the potential drop. This is the basic operation mode of water-TENG devices. However, the manner by which the tribo-charges are formed on the solid surface when interacting with water requires explanation. A recent explanation of the formation of tribo-charges was proposed by Zhong Lin Wang's group [20,21]. When water is not in contact with a solid surface, the water molecules are distributed in the water, and the virgin surface is without pre-existing charges (see Fig. 2a, schematic representation of molecules in solution). At this stage, the molecules/atoms in the water and atoms on the solid surface bind the electrons tightly in specific orbitals and stop them from escaping, as shown in Fig. 2d. Further, when the water molecules/atoms interact with the atoms on the solid surface, a strong overlap of electron clouds can be observed, as shown in Fig. 2b. At this stage, the energy barrier between the water molecules and the atoms on the solid surface is reduced, owing to the strong overlap of electron clouds. As shown in Fig. 2e, an electron transfers from one atom to another, resulting in contact electrification. In the next stage, when the water is pushed away by hydraulic pressure (Fig. 2c), the transferred charge remains on the solid surface as static charge (Fig. 2c and f). Simultaneously, the water is also charged. In addition, contact electrification between the water/solid surface and gas/air can also cause the water to be charged. This is the origin of the tribo-charges contributing to power generation in water-TENG devices. As water approaches a conductive surface covered by an insulative layer, electrostatic induction in the conduction layer generates a charge flow. This is the basic principle of water-based TENG devices.

The previous paragraph explains how tribo-charges are formed on a

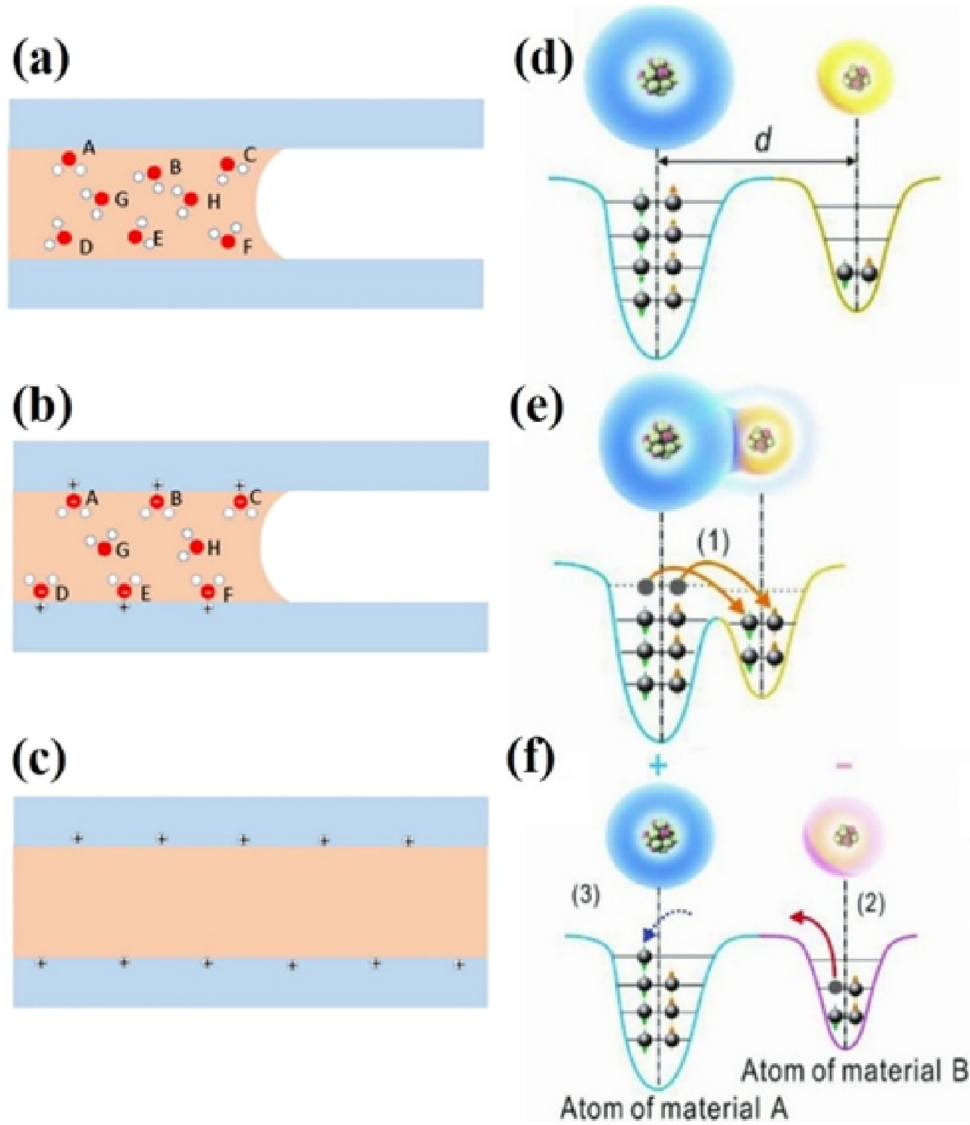


**Fig. 2.** Charge transfer mechanism when a solid surface interacts with water. (a) schematic illustration of water molecules; (b) water molecules/atoms interact with solid surface and contact electrification occurs; (c) water molecules are pushed by hydraulic pressure. Interaction between water and solid atomic molecular orbits before (b), during (e) and after (f) contact at a distance shorter than bounding length, which results in electron transfer. Reproduced with permissions [20], Copyright 2019, Elsevier.

solid surface when interacting with water. However, further discussion is required as to how these tribo-charges are converted into electricity. The output current of a water-TENG device originates from a displacement current induced by the varying polarisation field [10]. The displacement current was systematically postulated by Maxwell in 1861, in connection with the displacement of electric particles in a dielectric medium [22]. The displacement current is defined as follows:

$$J_D = \frac{\partial D}{\partial t} = \varepsilon \frac{\partial E}{\partial t} + \frac{\partial P_s}{\partial t} \quad (1)$$

Here,  $J_D$  is the displacement current,  $D$  is the electric displacement field,  $E$  is the electric field,  $P_s$  is the polarisation field arising from the surface charges contributed by either piezoelectric and/or triboelectric effects, and  $\varepsilon$  is the permittivity of the medium. There are two terms in the expression of displacement current. The first term is the contribution from the time-varying electric field, which originates the electromagnetic waves. The second term is the contribution from the time-varying polarisation field. When surface polarisation charges exist in a medium, e.g. piezoelectric or triboelectric materials, the polarisation density of the surface electrostatic charges cannot be ignored, and the

second term  $\partial P_s / \partial t$  in Equation (1) is the theoretical origin of the nanogenerators [23]. Fig. 2 explains the formation process of the tribo-charges on the solid surface when interacting with water. These tribo-charges build an electrostatic field, and drive electrons to flow through an external circuit. The current in the internal circuit is dominated by the displacement current, and the measured current in the external circuit is a capacitive conduction current. For the further derivation of a detailed expression for the current in a water-TENG device, one can assume two media with dielectric permittivities of  $\varepsilon_1$  and  $\varepsilon_2$  and thicknesses of  $d_1$  and  $d_2$ , respectively. If the triboelectricity-introduced surface charge density is  $\sigma_c(t)$ , and the density of the free electrons on the surface of the electrode is  $\sigma_1(z, t)$ , the electric fields in the two media and in the gap (height of  $z$ ) between the two media are:  $E_{z1} = \sigma_1(z, t) / \varepsilon_1$ ,  $E_{z2} = \sigma_1(z, t) / \varepsilon_2$ ,  $E_z = (\sigma_1(z, t) - \sigma_c) / \varepsilon_0$ . Here,  $z$  is the distance between the two media. The potential drop can be expressed as follows:

$$V = \sigma_1(z, t) [d_1 / \varepsilon_1 + d_2 / \varepsilon_2] + z [\sigma_1(z, t) - \sigma_c] / \varepsilon_0 \quad (2)$$

Under a short-circuit condition,  $V = 0$ , and the displacement current inside the medium can be derived as:

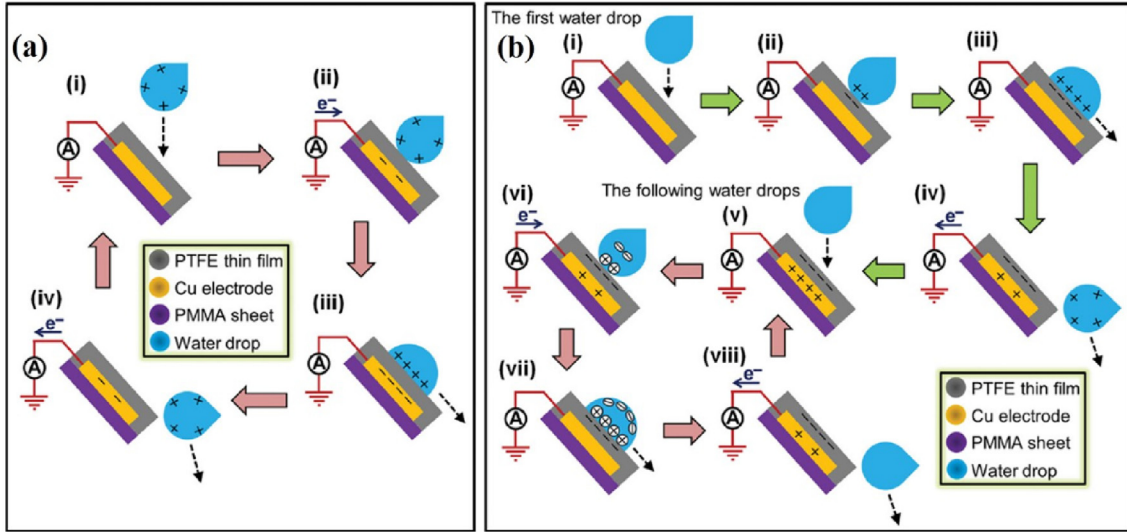


Fig. 3. Working principle of a single-electrode water-TENG device: (a) the water droplet and air/pipe contact electrification-dominated and (b) the water droplet and polytetrafluoroethylene (PTFE) contact electrification-dominated. Reproduced with permissions [24], Copyright 2014, Wiley-VCH.

$$J_D = \frac{\partial D_z}{\partial t} = \frac{\partial \sigma_f(z, t)}{\partial t} = \sigma_c \frac{dz}{dt} \frac{d_1 \varepsilon_0 / \varepsilon_1 + d_2 \varepsilon_0 / \varepsilon_2}{[d_1 \varepsilon_0 / \varepsilon_1 + d_2 \varepsilon_0 / \varepsilon_2 + z]^2} + \frac{d\sigma_c}{dt} \frac{z}{d_1 \varepsilon_0 / \varepsilon_1 + d_2 \varepsilon_0 / \varepsilon_2 + z} \quad (3)$$

In Equation (3), the first term describes that the magnitude of the displacement current is proportional to the speed at which the two media contact and separate ( $dz/dt$ ). The second term is related to the rate at which the surface charge density builds up. Typically, after 10 iterations of the contacting motion,  $\sigma_c$  reaches saturation, and the second term vanishes. With the contact and separation motions between water and TENG device, the formed tribo-charges can induce a current flow through the external circuit. The working principle of the water-TENG devices can be classified into three modes: single-electrode mode, sliding free-standing mode, and pressing-releasing mode.

### 2.1. Single-electrode mode

The working principle of a single-electrode-mode water-TENG device can be seen in Fig. 3 [24]. The device is made of stacked layers of poly (methyl methacrylate) (PMMA) substrate, a copper electrode, and polytetrafluoroethylene (PTFE) thin film. The copper electrode is connected to the ground through an external circuit. In the single-electrode mode, the origin of the triboelectric charge can arise from two sources: the triboelectric charge created when a water droplet moves in the air or in a pipe (as shown in Fig. 3a), and the charge created when a water droplet slides on the PTFE film, as shown in Fig. 3b. Depending on the significance of the respective contributions of the two origins, the mechanism could be separated into two parts: water droplet and air/pipe contact electrification-dominated, and water droplet and PTFE contact electrification-dominated. As shown in stage (i) in Fig. 3a, the water-TENG device is initially in electrical equilibrium, as the water droplet surface attains positive charges while transporting through the air or in a pipe. The origin of these positive charges could be attributed to the contact electrification phenomenon presented in Fig. 2. When the water droplet impacts on the tilted water-TENG device, an electrostatic induction process takes place, and the electrons are attracted from the ground to the copper electrode with the effect of Coulomb force, as shown in stage (ii) in Fig. 3a. After the impact motion, the water droplet spreads and induces a larger contact area with the water-TENG device, leading to a sharp increase in the current flow in the external circuit (stage (iii) in Fig. 3a). When the water droplet rolls off the PTFE surface, the induced electrons flow back to the ground as the Coulomb

force vanishes. It is noteworthy that the motion of a single water droplet (impact, spread, and roll off) will generate an alternating current as the direction of electron flow reverses.

The mechanism for the water droplet and PTFE contact electrification-dominated process is more complicated than the water droplet and air/pipe contact electrification. As shown in stage (i) in Fig. 3b, the water-TENG device is initially in electrical equilibrium, and the water droplet also exhibits electric neutrality. When the water droplet impacts the water-TENG device, owing to the contact electrification effect presented in Fig. 2, the PTFE layer reveals as negative. When the water droplet fully spreads on the surface, a large number of negative charges accumulate on the PTFE surface. Once the water droplet rolls off the water-TENG device as shown in stage (iv) in Fig. 3b, the negative charges remain on the PTFE surface, and an electron flow is induced with the effect of Coulomb force. From stage (i) to stage (iv), the current generation is induced by the first water droplet. The mechanisms for when subsequent water droplets impact on the negatively charged water-TENG surface are shown in stage s(v) to (viii). In stage (v), the negative charges on the PTFE surface are fully-compensated for by the positive charges in the copper electrode. When the second water droplet impacts the water-TENG device as shown in stage (vi), the cations are attracted to the droplet surface. As a result, the negative charges on the PTFE surface are compensated for by the attracted cations, while the copper electrode reveals excessive positive charges. An electron flow is induced from the ground to compensate for the excessive positive charges on the copper electrode. As shown in stage (vii), the water droplet fully spreads on the water-TENG device, and the negative charges on the PTFE surface are purely compensated for by the cations of the droplet. In stage (viii), a process identical to stage (iv) takes place, and a loop is induced if a third water droplet impacts the water-TENG device. The droplet and PTFE contact electrification-dominated process also induces an AC-type current signal.

### 2.2. Sliding free-standing mode

The sliding free-standing mode is another important power generation mode based on the sliding motion of a water droplet on a water-TENG device with pairs of electrodes [25]. The working principle of a sliding free-standing mode water-TENG is illustrated in Fig. 4 [15]. The dark blue, brown, yellow, red, and light blue colours represent the water droplet, hydrophobic layer, dielectric layer, the pair of electrodes, and substrate, respectively. The dielectric layer should be

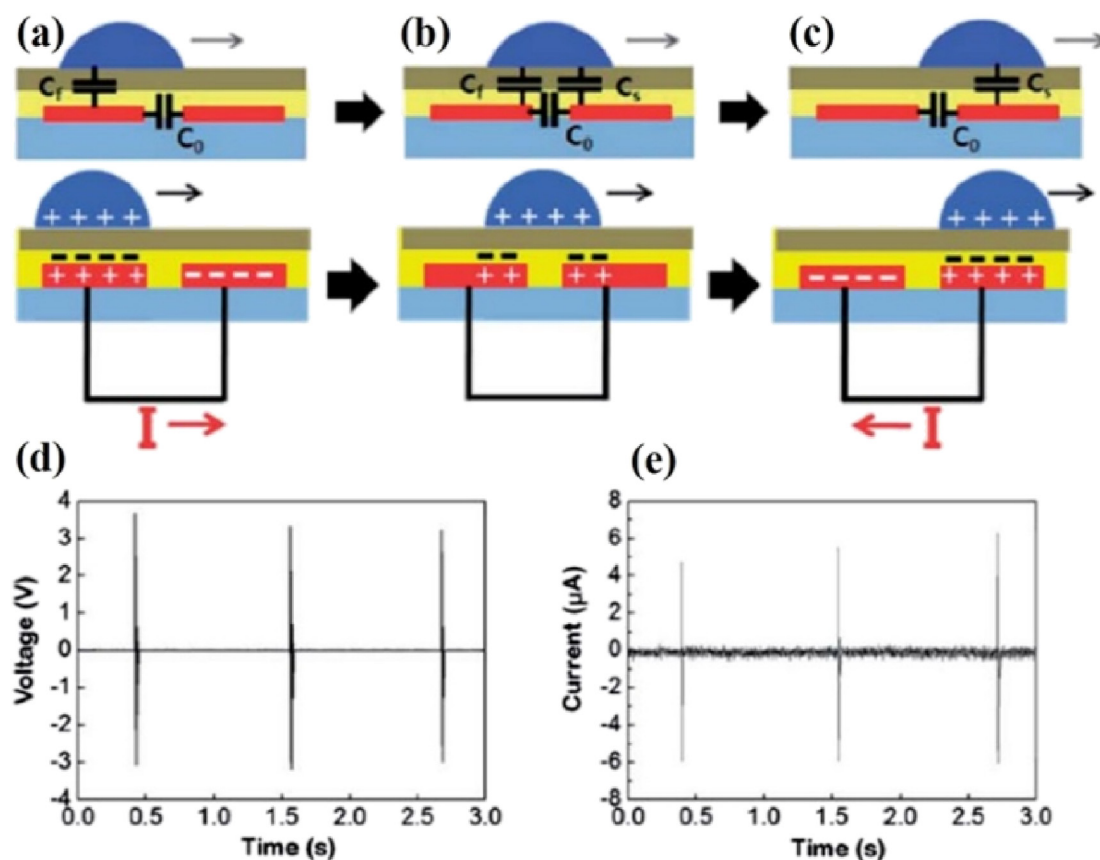


Fig. 4. Working principle of a sliding free-standing mode water-TENG (a–c) charges distribution and current flow induced by the droplet sliding motion, (d) and (e) open-circuit voltage and short-circuit current induced by the droplet sliding motion. Reproduced with permissions [15], Copyright 2014, Royal Society of Chemistry.

formed by a thin insulating material, e.g. poly-4-vinyl phenol (PVP). Similar to the situation with the single-electrode mode water-TENG device, the tribo-charges are formed on the dielectric and water surfaces. The positive charges on the water compensate for the negative charges of the PVP layer, and the positive charges on the electrode are revealed. These positive charges induce an electron flow from the second electrode to the first, and an electric current is generated. Similarly, as the water droplet moves to the region above the second electrode, the same process is repeated, and a current flow with the reverse direction can be generated. When a water droplet moves above the pair of electrodes, an AC-type current signal can be obtained. In this sliding free-standing mode, water in the form of raindrops, spray drops, etc. could be employed for triboelectrification and energy harvesting. In the example shown in Fig. 4d, once a 30  $\mu\text{L}$  water droplet slides down a pair of 7 mm width electrodes, a 3.1 V open-circuit voltage and a 5.3  $\mu\text{A}$  current were generated. This power output can light an LED bulb. Some other studies [26–28] have reported on droplet sliding motion-induced power generation by water-TENGs, and recorded a maximum open-circuit voltage of 46 V with an 80  $\mu\text{L}$  sliding droplet [29].

Apart from the direct impact motion of a droplet on a water-TENG device, enclosed structures [23,30,31] are also employed for harvesting water wave energy in a sliding free-standing mode. Fig. 5a [32] presents a real picture of a lab-scale enclosed-structure TENG device. It is composed of a transparent sphere, aluminium electrodes, a Kapton layer, and an inner nylon ball. As shown in Fig. 5c, when the entire sphere is driven by a water wave, the nylon ball rotates inside the sphere. The rotating motion leads to contact and separation with the Kapton film above the two Al electrodes. Similar to Fig. 4, such a motion induces charges to transfer between the electrodes, and to contribute to an AC-type current signal. Fig. 5d and e presents the

transferred charges and open-circuit voltage of the enclosed free-standing mode TENG device, respectively. Owing to the large surface charge density of the solid materials [20], the enclosed TENG devices typically provide a larger output performance than the water-solid TENG devices. Moreover, the enclosed structure seals the TENG and prevents moisture penetration, which is also favourable for high-output performance [33]. However, the enclosed structure has challenges insofar as complexity and higher costs during fabrication.

### 2.3. Pressing-releasing mode

The pressing-releasing mode water-TENG is also important for harvesting energy from water motion. Compared to a single-electrode and sliding free-standing mode water-TENG, which generates electricity from water motion (droplets falling down and water waves), a pressing-releasing type water-TENG can be driven by any reciprocating movement. As shown in Fig. 6a [34], a pressing-releasing mode water-TENG is formed by one piece of PTFE-coated indium tin oxide (ITO, although it could be replaced by another conductive material) glass, one piece of ITO-coated glass, a water bridge, and an external load resistor. As shown in Fig. 6c, owing to the hydrophobicity of the PTFE material, the droplet has a smaller contact area with the top plate. Conversely, a much larger contact area is obtained between the water bridge and the ITO surface, which is hydrophilic. Electrostatic double layers (EDLs) are formed on both sides of the water bridge, and behave like serially-connected capacitors. With an external pressing motion on the bottom plate as shown in Fig. 6d, the contact area between the water bridge and top plate is increased, and a part of the cations moves towards the top plate to compensate for the negative charges. The change of the cations' distribution in the water bridge induces an electron flow from the bottom plate to the top plate through an external circuit, and a

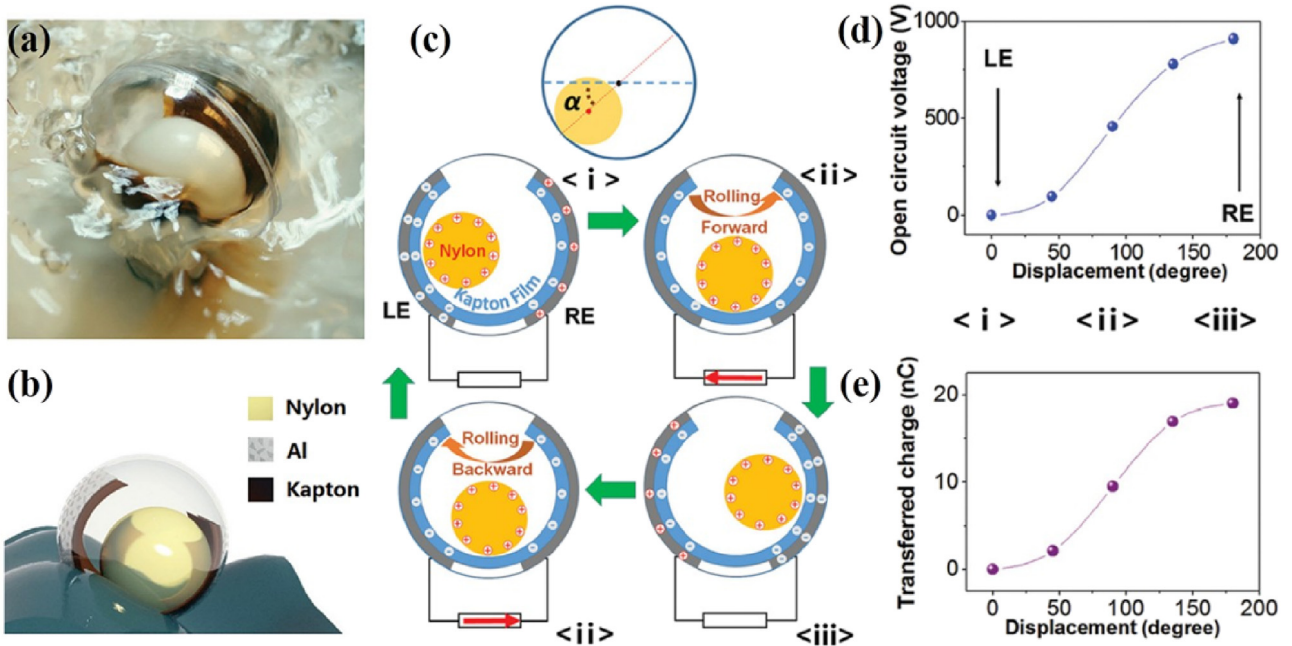


Fig. 5. Structure, working principle, and output performance of free-standing mode enclosed TENG device for harvesting the water wave energy. Reproduced with permissions [32], Copyright 2015, Wiley-VCH.

current signal is generated. Similarly, if a releasing motion is applied, the device moves to its initial position. As a result, the cations move back to the original state, and a reverse current is obtained through the external load resistor. With a pressing-releasing motion, an alternating current can be measured through the load resistor. A resistor-capacitor model can be employed to describe the voltage and current flow of the pressing-releasing mode water-TENG. The simplified circuit model is shown in Fig. 6c. The top EDL is represented by a capacitor with the voltage  $Q_T/C_T$ . Similarly, the bottom capacitor also possesses a voltage of  $Q_B/C_B$ .  $R_F$  is the resistance of the water bridge, and  $R_L$  is the resistance of the load resistor. Once a pressing motion is applied to the bottom plate, the updated circuit is shown in Fig. 4d. The contact area between the water bridge and bottom plate remains the same, but the contact area between the water bridge and top plate is increased. The circuit at moment  $t$  could be expressed in Equation (4):

$$(R_F + R_L) \frac{dq(t)}{dt} = V_B(t) - V_T(t) = \frac{Q_B - q(t)}{C_B} - \frac{Q_T(t) + q(t)}{C_T(t)} \quad (4)$$

Equation (4) is derived from Ohm's law. The left side of Equation (4)

represents the current flow multiplied by the total resistance. In that regard,  $dq(t)/dt$  is the charge variation at the moment of  $t$ , which contributes to the current flow.  $(R_F + R_L)$  represents the total resistance in the circuit. The middle part of Equation (4) is the voltage variation at the moment of  $t$ .  $V_B(t)$  is the voltage on the bottom plate, whereas  $V_T(t)$  represents the voltage on the top plate. The right side of Equation (4) is the detailed explanation of  $V_B(t)$  and  $V_T(t)$  at the moment of  $t$ . The bottom electrode loses  $q(t)$  number of charges, whereas the top electrode attains the  $q(t)$  number of charges. At the same time, the capacitance on the bottom plate remains the same, whereas the top plate capacitance changes as  $C_T(t)$ , owing to the contact area variation. The charge movement does not stop until  $V_B = V_T$ .

A water-TENG device with a pressing-releasing working mode could be employed for harvesting mechanical energy from a footprint [35]. With a total area of  $40 \text{ cm}^2$ , which is  $1/4$  of the area of a human footprint, the device is estimated to produce 2 W of power under a 10 V bias voltage.

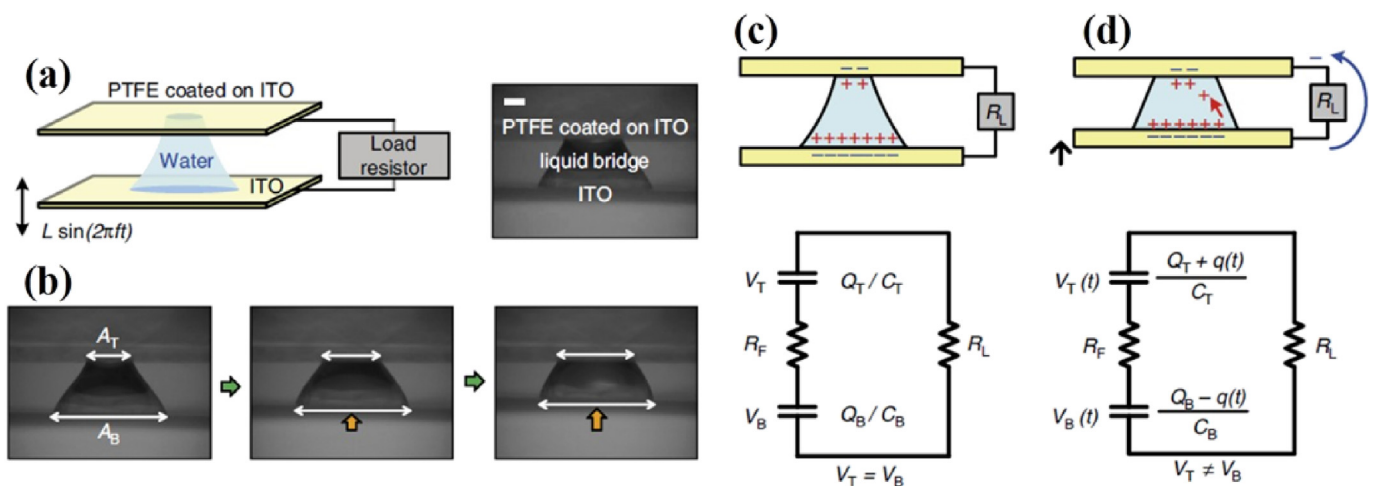


Fig. 6. Working principle of pressing-releasing mode water-TENG device. Reproduced with permissions [34], Copyright 2013, Springer Nature Publishing AG.

## 2.4. Affecting parameters

In the aforementioned types of water-TENG devices, the major components are as follows: the TENG device, water (either in the form of droplets, waves, or streams), and the external circuit. There are many factors affecting the output performance of the water-TENG devices. These can be classified as: TENG device properties, water properties, and the dynamic interaction between the water and the water-TENG device.

### 2.4.1. Design of triboelectric nanogenerator (TENG) device

There are two major parts of the water-TENG devices (of any working modes), *i.e.* the electrodes and hydrophobic coatings. Aluminium, ITO, and copper are typical electrode materials for water-TENG devices, as well as other solid-based TENG devices [36–38]. This could be attributed to the high electrical conductivity, low cost, and good flexibility of such materials [39]. In some applications that require transparent electrodes, such as a raindrop/solar hybrid harvesting system, ITO electrodes are preferred, owing to their low attenuation coefficient for incident light. In recent years, some carbon-based materials have been proposed, including carbon nanotubes (CNT) [40], graphene [41], and carbon nanosheets [42], owing to their high electrical conductivity and large contact area. These electrodes are widely employed in solar cells, lithium-ion batteries, and supercapacitors. The high conductivity and large contact areas of carbon-based electrodes are also favourable in water-TENG devices. However, investigations on carbon electrode-based TENGs are rarely reported. In terms of the configuration of the electrodes, interdigital designs have been proposed for a sliding free-standing mode droplet-TENG device, as shown in Fig. 7a [43,44]. With the multiple pairs of electrodes, the output voltage signal has multiple peaks and troughs during one droplet sliding cycle (Fig. 7b), and the number of the peaks is comparable with the number of electrodes. Typically, a device with an interdigitated electrode (IDE) design is connected with a full-wave rectifier for converting the negative peaks into positive peaks.

Another important component of a water-TENG device is the hydrophobic layer. The constituent materials of the hydrophobic layer are typically PTFE and fluorinated ethylene propylene (FEP). These two materials are commonly employed in TENG devices owing to their high affinity to negative charges. In a triboelectric series, the PTFE and FEP materials are most-negatively charged. The surface charge density is employed to evaluate the performance of a material. The FEP layer is reported with a surface charge density of 16–42  $\mu\text{C}/\text{m}^2$  [18,36], and the water droplet is measured with a surface charge density of 4.5  $\mu\text{C}/\text{m}^2$  when released from a PTFE tube [45]. It is noteworthy that there are techniques for increasing the surface charge density of the FEP and

PTFE hydrophobic layers. One of the techniques is the single-polarity charged ions injection method [46]. The single-polarity charged ions injection method is performed using an air ionisation gun. The surface charge density of the FEP thin film is boosted from 50 to 250  $\mu\text{C}/\text{m}^2$  after the ionisation gun treatment. A recent method [47] using an external and self-charging excitation scheme boosted the effective surface charge density of up to 1.25  $\text{mC}/\text{m}^2$ . In addition to the surface charge density, the hydrophobicity is also a vital parameter affecting the performance of a water-TENG device. When water is interacting with the TENG surface, an adhesion force is a major resistive force applied to the water (in the form of either a droplet or water flow). Lin et al., [24] comprehensively compared the output performance of a single-electrode-mode TENG device with varied hydrophobicities: a superhydrophobic PTFE thin film with hierarchical micro-/nano structures, a plain PTFE hydrophobic thin film, and a nylon hydrophilic thin film. The results revealed that the output performance follows a trend of  $I_{\text{superhydrophobic}} > I_{\text{hydrophobic}} > I_{\text{hydrophilic}}$ . This is because on a superhydrophobic surface, a droplet first spreads out, and then easily bounces off the surface within a short duration [48]. The droplet spread area on the superhydrophobic surface is smaller than that on the hydrophobic or hydrophilic surface [49], which adversely affects power generation. The result in Ref. [24] indicates that the velocity increment is a dominant effect in current generation, as compared to the adverse effect induced by the reduction in contact area. The superhydrophobic surface was prepared by pouring PTFE precursor into an anodic aluminium oxide (AAO) template. A PTFE layer with hierarchical micro-/nano structures can be peeled off once it is cured. Other methods for preparing a PTFE- or FEP-based superhydrophobic surface have also been reported, including thermal nanoimprinting [50], inductively-coupled plasma etching [51], and conformal fluorine coating on carbon electrodes with micro-/nano structures [52]. It is noteworthy that a superhydrophobic surface is favourable for obtaining a high current output in the single-electrode working mode. This is because the superhydrophobic surface not only provides the fast motion of droplets, but also enables a complete rebound of the droplet within certain impact velocities [48]. For the sliding free-standing and pressing-releasing working modes, the scenario might be different, as the sliding area is also a very important factor in current generation. More detailed studies should be conducted to suggest a proper hydrophobicity for the sliding free-standing and pressing-releasing mode TENGs.

### 2.4.2. Water property

As a water-TENG device can be used for harvesting hydropower from different sources, the properties of water in the forms of raindrops, ocean waves, and flowing rivers should be considered. Some major properties of water include the ion type and concentration. A

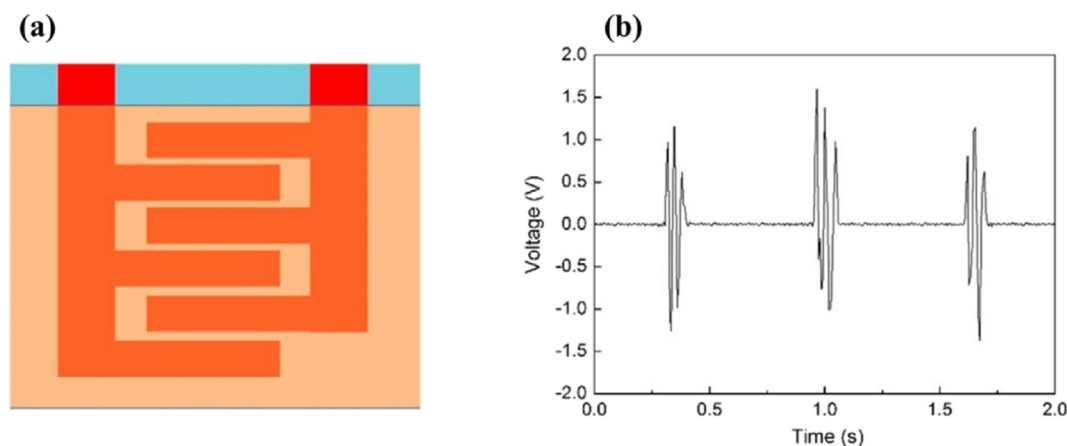
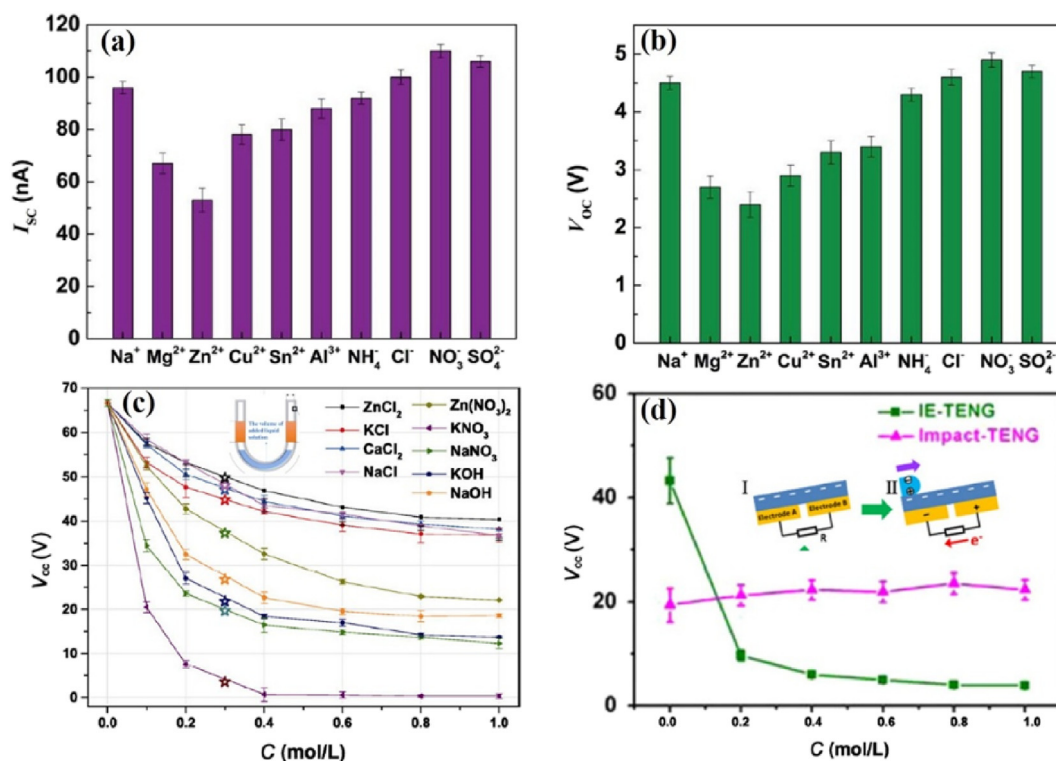


Fig. 7. (a) Schematic of TENG device with an interdigitated electrode (IDE) design and (b) open-circuit voltage obtained by the TENG device with IDEs. Reproduced with permissions [43], Copyright 2015, American Chemical Society.



**Fig. 8.** Effects of ions' type and concentration on water-TENG device. (a) and (b) effect of ions' type, Reproduced with permissions [54], Copyright 2017, Wiley-VCH. (c) and (d) effect of ions' concentration. Reproduced with permissions [27,53], Copyright 2018, Springer Nature Switzerland AG, Copyright 2014, Elsevier.

comprehensive investigation on ion properties was carried out in a single-electrode mode flow-stream TENG. Standard solutions with different types of ions were tested. As shown in Fig. 8a and b, the short-circuit current and open-circuit voltage are varied when different types of ions are applied. The effect of ion type on the output performance of the TENG can be attributed to two causes. First, the electronegativity of ions affects the output performance of the TENG. This is because ions with low electronegativity values prefer to absorb the  $F^-$  groups of the FEP or PTFE hydrophobic layers, which is harmful to the output performance of the TENG [53]. Second, the electrical conductivity of the ions also contributes to the output performance of the TENG device [54]. A higher electrical conductivity would lead to a reduced output performance. This is because the high conductivity ions contribute less to the amount of triboelectric charges on the hydrophobic layer. This could also be explained by the mechanism presented in Fig. 2c. The tribo-charges are formed on the solid surface after the occurrence of contact electrification, and these tribo-charges would screen the electrons on the back electrode and contribute to the current flow in the water-TENG devices. If a high ion concentration exists in the aqueous solution, these ions could be attracted by the tribo-charges. In contrast, part of the tribo-charges would be compensated for by the ions. The reduced amount of triboelectric charges induces a less-significant electrostatic induction effect, and yields a decreased output current and voltage. In terms of ion concentration, several studies [27,53] have shown that an increase in ion concentration would reduce the output performance of the TENG. As shown in the inset of Fig. 8c, a liquid/FEP U-tube TENG device is proposed for harvesting water wave energy. The effects of ion concentration on the output performance are examined, and the open-circuit voltage is found to reduce with an increase of ion concentration from 0 to 1 mol/L. This decreasing trend was found in different types of salt solutions, as shown in Fig. 8c. A liquid-solid based TENG device, as a self-powered distress signal emitter, is presented in the inset of Fig. 8d. The liquid/FEP thin film forms an interfacial contact electrification triboelectric nanogenerator (IE-TENG), whereas the nanostructured PTFE and elastic wavy electrode form an impact-TENG.

The impact-TENG operates with a solid-solid contact-separation working mode. The results indicate that with an increase of NaCl concentration, the performance of the IE-TENG drops significantly. However, the impact-TENG maintains its output current. This is because the impact-TENG works by solid-solid interaction, which is not influenced by the ion concentration.

The pH value is another important property of water. Owing to different contents in the water, the pH value varies from 5.0 to 9.0 in the Yangtze River [55]. A pH detector was fabricated, based on the output voltage difference when using water with varied pH values. A decreasing trend was obtained when the pH value decreased from 7.0 to 2.0, as shown in Fig. 9a [56]. As the low pH-value solution contains more  $H^+$ , it can render the cations in the electrolyte solution. As a result, the anions have difficulty passing through the interface, and the concentration of triboelectric charges on the hydrophobic layer is reduced. The temperature of water also affects the output performance of the TENG device [57]. As shown in Fig. 9b, the output current density continuously decreases with increases of water temperature. This is because the dielectric constant and polarity of water decrease with an increase of temperature [58], which weakens the output performance of the water-TENG. It should be noted that the viscosity and surface tension would also be affected by water temperature. The change in viscosity and surface tension would change the contact area between the water and TENG devices. According to Equation (3), the output current of the water-TENG would be firmly changed if the contact area between the water and TENG surface is varied. In that regard, intensive studies on droplet spread dynamics varying with droplet properties have been conducted [48,59]. However, a systematic investigation of the effects of viscosity and surface tension on the output performance of a water-TENG device is lacking.

#### 2.4.3. Dynamic interaction between water and TENG device

The interaction between the water and the water-TENG device plays an important role for power output. It is known that the output current is proportional to the contact area  $A$  and the variation of induced

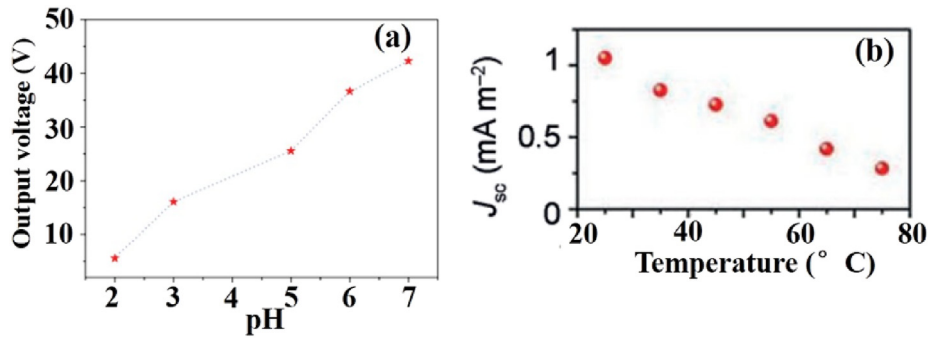


Fig. 9. (a) Effects of pH value on the output performance of TENG, Reproduced with permissions [56], Copyright 2016, Hindawi, and (b) effects of liquid temperature on the output performance of TENG. Reproduced with permissions [57], Copyright 2013, Wiley-VCH.

charges with respect to time. Further, it can be seen that a larger contact area and higher flow speed are beneficial for obtaining a high power output. A comprehensive investigation on the droplet volume, initial height, and tilting angle was conducted on a sliding free-standing mode water-TENG device [28]. The output current is linearly proportional to the initial height of the water droplet. This is because the current is proportional to the square of the velocity, according to Correlation 5:

$$I \propto \sigma \frac{dA}{dt} \propto \sigma \left( \frac{\rho D^3}{\gamma} \right)^{1/2} v^2 \quad (5)$$

This correlation can be derived when a droplet is impacting on an inclined surface. It is derived that the output current is proportional to the surface charge density multiplied by the contact area variation with respect to time. In the middle part of Correlation 5, the contact area variation with time is dependent on the hydrodynamics of the droplet. Before contact with the inclined surface, the droplet is estimated as a sphere with a diameter of  $D$  and velocity of  $v$ . During the droplet impact process, the droplet is compressed, and the velocity decreases to zero. The inertial force (per volume) applied to the droplet can be expressed as  $\rho v^2/D$ . As the momentum energy of the droplet is dissipated by the surface tension, a force balance can be established between the inertial force and the Laplace pressure gradient:  $\rho v^2/D \sim \gamma/t^2$ . By substituting the term  $dt$  into the middle part of Correlation 5, one can obtain the right-side expression. It is noteworthy that this correlation only describes the process before the droplet impacts onto the surface, and until it is fully spread. Subsequent retraction and sliding motions are not considered in this case. In Correlation 5,  $D$  is the diameter,  $\rho$  is the density,  $\gamma$  is the surface tension, and  $v$  is the velocity of the droplet. According to energy conservation,  $mgh = \frac{1}{2}mv^2$ , a linear relationship could be derived as  $I \propto h$ . With an increase of the inclination angle of up to  $45^\circ$ , the output current increases, and this could be attributed to the acceleration effect of the water droplet on the highly-inclined surface. However, when the angle exceeds  $45^\circ$ , the output current reaches saturation. This could be caused by the reduced contact area when a droplet is impacting on an inclined surface. The single-electrode and sliding free-standing mode water-TENG devices could be simplified as a droplet impact process integrated with a triboelectrification process. When a droplet is impacting on an inclined surface, the droplet would experience spread, recoil, deposit, sliding, rebound, or splash according to its initial state, as well as the surface property [60]. The droplet spread is mainly determined by inertia, whereas the following recoil, deposit, sliding, rebound, and splash motions are typically governed by the wettability of the surface. A superhydrophobic surface possesses a low surface energy, allowing for a fast droplet motion on the water-TENG surface. However, when a droplet impacts on a superhydrophobic surface, the recoil process happens quickly, and the rebound and splash phenomena are typically observed. Moreover, if a droplet is impacting at a high Weber number condition, it will penetrate into the air pockets on the superhydrophobic surface, and yield a

deposition [61]. These phenomena generate adverse effects for the water-TENG devices. The water dynamics play an important role in the output performance of a water-TENG device. However, previous studies have paid relatively less attention to the effects of water dynamics on the output performance of a water-TENG device. Investigations on the water-TENG devices with functional surfaces (wettability gradient surface [62], hydrophobic/hydrophilic heterogeneous surface) should be conducted, as the droplet motion could be dynamically tuned on these surfaces.

### 3. Applications in energy harvesting devices

Hydropower widely exists in nature, industry, and human daily life, in form of droplets, tides, waves, and river flows. Based on the mechanisms presented for the single-electrode, sliding free-standing, and pressing-releasing modes, various energy harvesting devices for converting hydropower into electricity have been developed.

#### 3.1. Harvesting energy from water wave

A group of water-TENG devices for harvesting water wave energy have been developed [51,53,63]. Water-TENG devices working in single-electrode mode or in sliding free-standing mode are suitable for harvesting water wave energy. Fig. 10a presents the concept of using a sliding free-standing mode water-TENG device for harvesting water wave energy. In this device, multiple pairs of electrodes were fabricated on top of a flexible substrate. A conductive textile was employed as the electrode material, and a dry-etched PTFE film was used for the hydrophobic coating. The whole device was 100 mm in length, and 70 mm in width. The output performance of the water-TENG is illustrated in Fig. 10b. With an increase of load resistance from  $10^4 \Omega$  to  $10^9 \Omega$ , the current decreased from  $14 \mu\text{A}$  to zero. In contrast, the voltage increased from close to zero to nearly 300 V. A peak power of 1.03 mW was obtained at a load resistance of 22 M $\Omega$ . With the harvested power, the authors demonstrated a wireless self-powered transmission of important hydrological information. The harvested water wave power was also employed to light up 60 LED bulbs in Ref. [18]. This could be an effective way for harvesting the water wave energy, as the water-TENG device provides advantages of flexibility, low cost, light weight, and being free of rotating parts.

#### 3.2. Harvesting energy from raindrops

Another important hydropower source is the raindrop. Similar to the water wave-harvesting water-TENGs, the devices for harvesting raindrop energy also operate in the single-electrode mode or sliding free-standing mode. The raindrop energy-harvesting devices are presented either alone on the surface of an umbrella, or in combination with silicon based, dye-sensitized, or quantum-dot solar cells [64–68]. They could also be employed for harvesting solar, wind, and raindrop

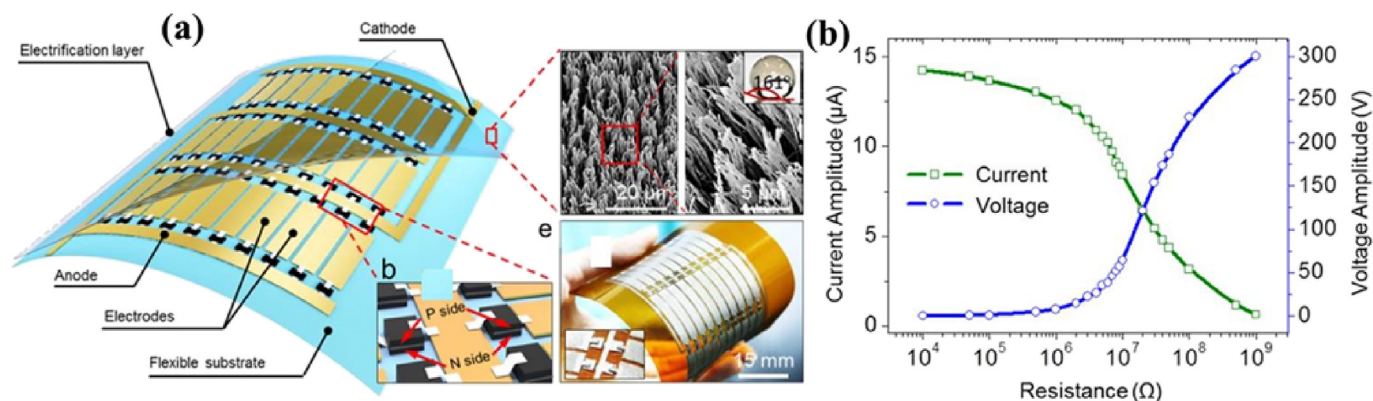


Fig. 10. (a) Concept of using sliding free-standing mode TENG device for harvesting water-wave energy and (b) output current and voltage of the water-TENG when harvesting water waves. Reproduced with permissions [51], Copyright 2018, American Chemical Society.

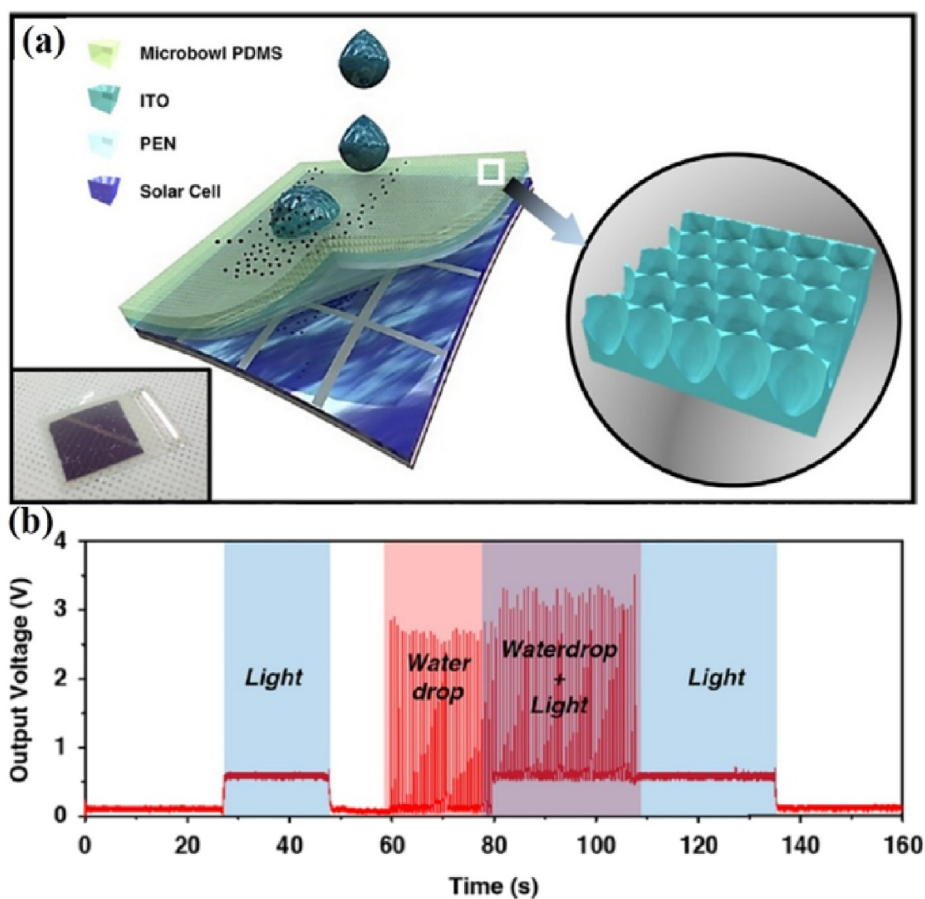


Fig. 11. A hybrid water-TENG and solar cell energy harvester. (a) schematic of the hybrid energy harvester and (b) output voltage characteristics working under different conditions. Reproduced with permissions [65], Copyright 2015, Elsevier.

energy as a hybrid cell [69]. Fig. 11a presents the concept of an integrated energy conversion unit for converting solar energy during a sunny day, and harvesting raindrop energy in rainy weather. The device is fabricated as a stacked water-TENG device integrated with a piece of a silicon-based solar cell. The water-TENG device is constructed to be thin and transparent, so that the sunlight could transmit and excite the solar cell for power generation. The water-TENG has a size of  $1 \text{ cm} \times 1 \text{ cm}$ , and the effective area of the solar cell is  $0.7 \text{ cm}^2$ . To enhance the output performance of the water-TENG device, a microbowl structure was fabricated on a polydimethylsiloxane surface, and a superhydrophobic property was achieved. The superhydrophobic surface not only enhances the droplet sliding speed on the water-TENG surface, but

also provides a self-cleaning effect for the solar cell when the surface is contaminated. As shown in Fig. 11b, when the hybrid cell is purely working under sunlight (solar simulator:  $150 \text{ mW/cm}^2$ ), approximately  $0.6 \text{ V}$  is obtained. When the device is driven by sequential water droplets, approximately  $2.7 \text{ V}$  can be attained. By simultaneously impacting water droplets and sunlight onto the device, both the water-TENG and solar cell maintain their output performance.

### 3.3. Harvesting energy from flowing stream

A flowing stream is another important type of hydropower resource. It typically appears in the forms of rivers, pipe flows, and so on. Single-

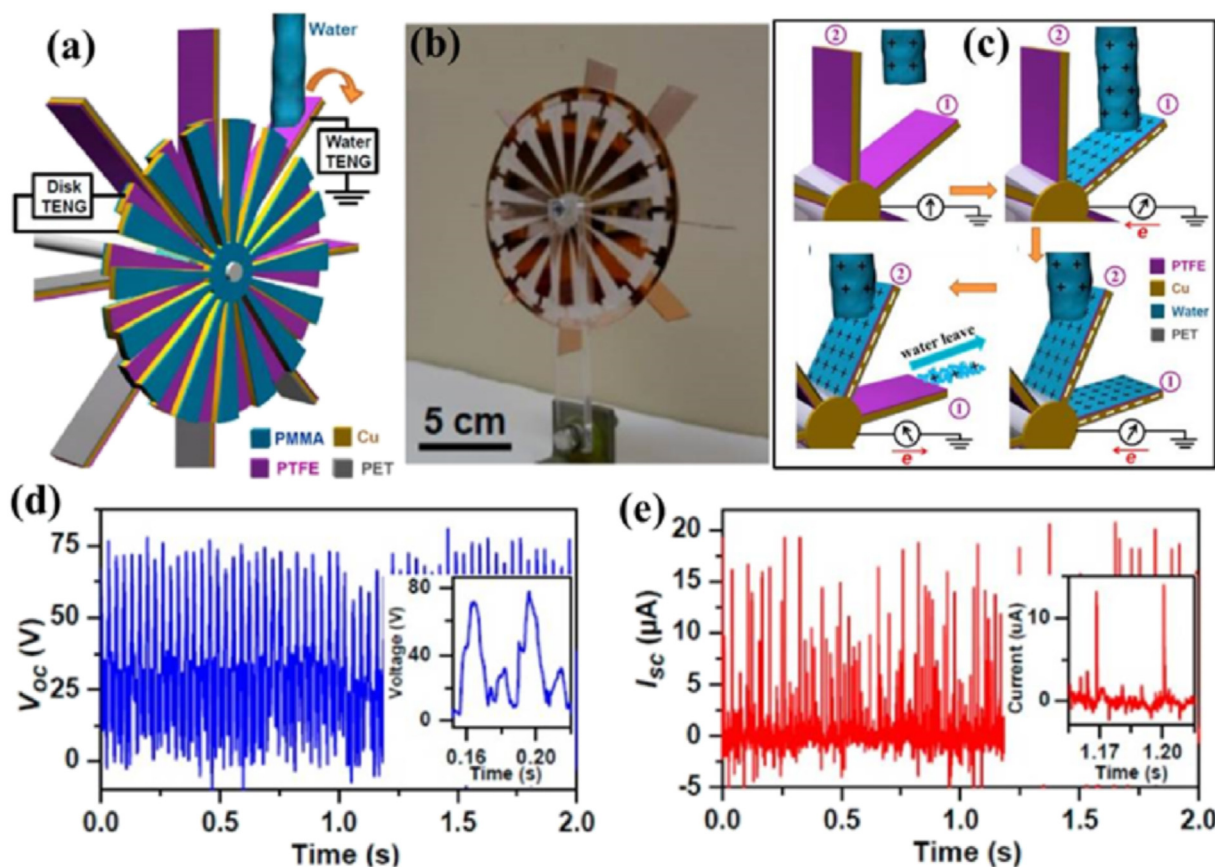


Fig. 12. (a) schematic of water-TENG device for harvesting the flowing river, (b) prototype of the water-TENG, (c) working principle of the water-TENG device, (d) and (e) open-circuit voltage and short-circuit current of the water-TENG during energy harvesting. Reproduced with permissions [17], Copyright 2014, American Chemical Society.

electrode mode and sliding free-standing mode water-TENGs are usually designed for harvesting the triboelectrification energy from a water stream [17,52,70,71]. Fig. 12 presents the concept of a single-electrode mode water wheel-type TENG. The device has a plate at the centre, and 8 blades attached. The configuration is the same as a water wheel for milling and hamming. A prototype of the water-TENG device is fabricated, and the scale bar in Fig. 12b indicates a length of 5 cm. The hydrophobic layer of the water-TENG is constructed with nanostructured PTFE. The working principle of this water-TENG device is presented in Fig. 12c, and is the same as the mechanism shown in Fig. 3a. When a stream of flowing water hits the surface of the water-TENG, the wheel is rotated, and the water leaves the blade under gravitational force. With the water impacting and leaving motions, an AC-type current signal can be obtained. An open-circuit voltage of 75 V and a short-circuit current of more than 12.9  $\mu\text{A}$  were measured. When the external load resistance increased to 88 M $\Omega$ , a maximum power of 0.24 mW was obtained. Another sliding free-standing mode water-TENG is presented [52] with a pair of conformal fluorine-coated carbon paper electrodes. The fluorine layer was employed for providing a hydrophobic property, and the carbon paper was used for its high electrical conductivity and rough structure on the surface. A superhydrophobic device was demonstrated for harvesting the hydropower from flowing water, and 5.3  $\mu\text{W}$  output power was achieved.

#### 4. Applications in self-powered sensors and actuators

The previous section reviewed water-TENG devices for harvesting hydropower in terms of raindrops, water waves, and water streams. The harvested energy is stored, and is typically employed for charging a commercial capacitor. In this section, the energy harvested by water-

TENG devices are directly consumed by sensors and actuators, as self-powered systems [72–74]. A group of self-powered sensors has been developed based on a water-TENG device for sensing, e.g. a distress signal [27], ethanol concentration [75], biological/chemical response [54], flow speed [38], wave height [76], or gas flow [77].

##### 4.1. Self-powered distress signal emitter and ethanol sensor

Fig. 13a–c presents the concept of using a water-TENG/impact-TENG hybrid device as a self-powered distress signal emitter [27]. The device has dimensions of 15 cm  $\times$  6 cm  $\times$  0.8 cm. A 75  $\mu\text{m}$ -thick FEP film was employed as the hydrophobic layer. During operation, the TENG device provides an open-circuit voltage of over 40 V. The system could be used for self-powering up to 48 commercial LEDs, which eliminates the discharge duration problems induced by chemical batteries. As shown in Fig. 13c, a man is floating on a river with a life jacket equipped with the TENG-based distress signal emitter. The LED lights keep shining, and a self-powered distress signal is emitted. The water-TENG device could also be utilised for sensing an ethanol concentration. As shown in Fig. 13d–f, a water-TENG device with a PTFE surface was fabricated with an effective area of 5 cm  $\times$  5 cm. When a water droplet was dripped onto the device, the droplet contact angle was close to 110°, and an open-circuit voltage of up to approximately 60 V was detected. However, when an ethanol droplet was dripped onto the surface, the open-circuit voltage was close to zero. This could be attributed to the spread area of the two types of droplets during dripping. When the ethanol droplets drip onto the water-TENG device, owing to a much smaller contact angle, a liquid film is easily formed on the PTFE surface, which shields the triboelectric charges and reduces the triboelectrically-charged area. With this scheme, the TENG device is

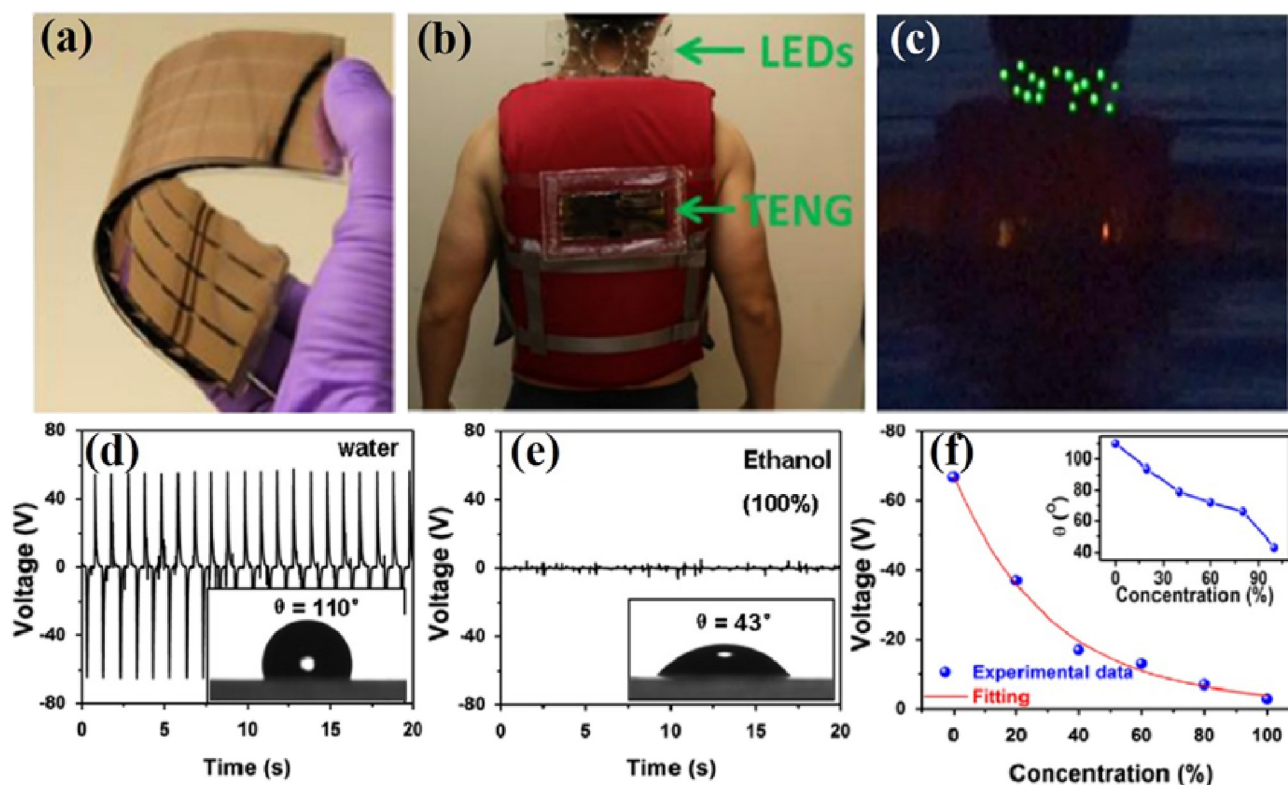


Fig. 13. Water-TENG devices as sensors for: (a–c) distress signal and (d–f) ethanol concentration. Reproduced with permissions [27,75], Copyright 2014, Elsevier.

employed as the ethanol concentration sensor. As shown in Fig. 13f, the output voltage continues to decrease with increases of ethanol concentration in water. The concentration of ethanol in a test solution could correspondingly be read out using the output voltage.

#### 4.2. Self-powered water quality sensor

Fig. 14 presents the concept of a water-TENG-based water quality sensor. The water-TENG device is formed by an ultrafine capillary PTFE tube, an aluminium foil electrode, and a silicon rubber tube working as a heat sink. The device operates under the single-electrode mode. The PTFE tube has an inner diameter of 0.5 mm, and a wall thickness of 0.25 mm. The aluminium electrode is in a double-helix shape with a width of 1 mm and a thickness of 0.1 mm. The quality of the barrelled drinking water was initially tested by a colony-counting method, as shown in Fig. 14b. It could be seen that the total aerobic count (TAC) increased exponentially with an increase of storage duration. After day 7, the TAC exceeded 110 cfu/ml, which is beyond the standard drinking water quality. Influenced by the TAC, the total dissolved solids (TDS) value also increases with the increased storage duration. The water samples were tested by the water-TENG device in a capillary tube, and the output performance is shown in Fig. 14d. It is seen that the short-circuit current, open-circuit voltage, and transferred charges all show a decreasing trend when the storage duration increases. This is because the electrolyte concentration in the drinking water continues to increase, weakening the output performance of the water-TENG. By this scheme, the water-TENG was employed as a self-powered water quality sensor.

#### 4.3. Self-powered wave monitoring

Wave monitoring is another important application for using water-TENG devices as self-powered sensors. This is because the sensing of ocean waves is essential for marine engineering construction and operations. A water-TENG-based wave monitoring system not only could

be used for sensing waves for avoiding disasters, but also to reduce the power consumption of isolated marine platforms, as a self-powered sensing system. Some self-powered water-TENG devices for sensing water levels and waves have been proposed [76,78]. Fig. 15a presents the concept of a water-TENG-based wave sensor. A lab-scale water-TENG device was fabricated with a size of 5 mm  $\times$  100 mm, and the surface of the water-TENG device was covered with an inductively-coupled plasma-treated PTFE film. With a wave motion, the single-electrode mode TENG device was triggered, and the output voltage could be measured for sensing the wave height. The variations in the height and frequency of the wave can be directly read out from Fig. 15b and c. With a fixed electrode width of 10 mm, the authors found that the output voltage linearly increases with the height, and a relationship of 23.5 mV/mm was given for linking the wave height and the detected voltage.

#### 4.4. Water-TENG enabled actuators

In addition to applications for self-powered sensors, applications for actuators have become increasingly attractive in recent years, owing to the rapid development of robots [79], controlled drug releases [80], micro-optics [81], micro-fabrication [82], and so on. Various TENG-based actuators have been developed based on the solid-solid triboelectric phenomenon [83–85]. However, owing to the relatively lower output voltage of water-TENG devices, applications using water-TENG devices for actuators are relatively scarce. Fig. 16 presents the concept of using a droplet-based TENG device for a self-powered digital microfluidics system [29]. As shown in Fig. 16a, the system is formed by an inclined sliding chip and a flat actuation chip. There are two pairs of electrodes on each chip. When a water droplet slides on the inclined surface, the contact electrification phenomena is triggered, and the left electrode of the sliding chip attains negative charges. Thus, the electrode of the actuation chip possesses excessive positive charges, as shown in Fig. 16c. As the right-side electrode is not affected by the sliding droplet, an electric potential is built up between the left- and

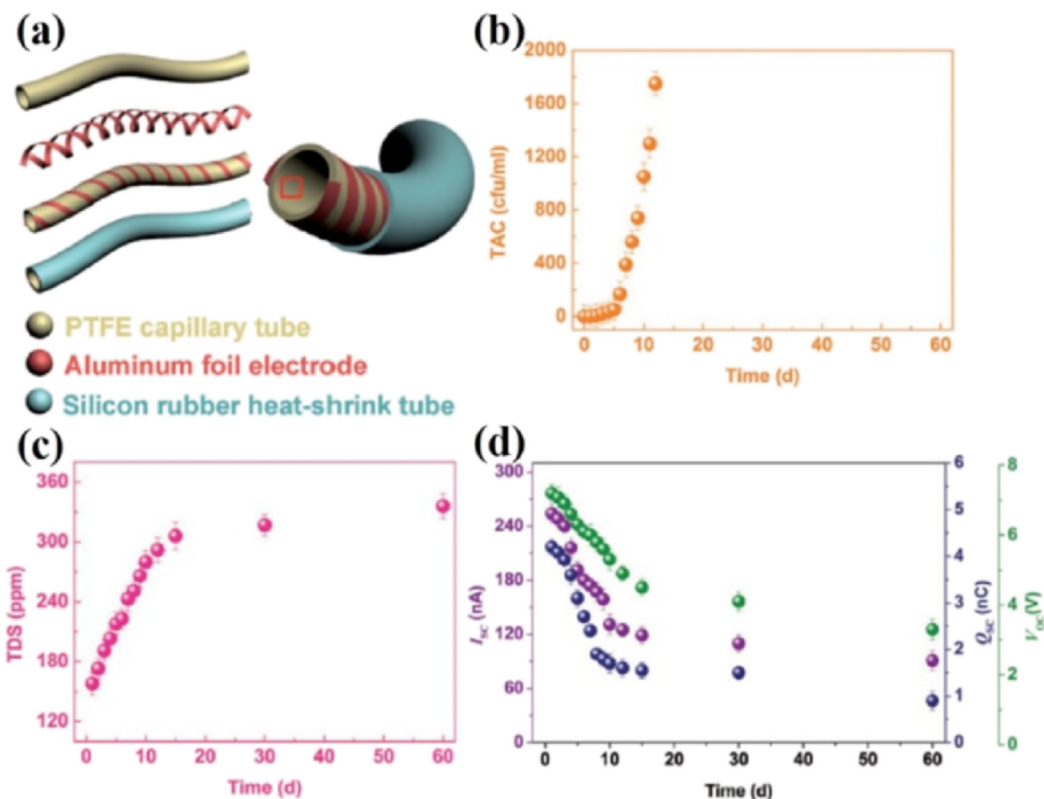


Fig. 14. Water-TENG based self-powered drinking water quality sensor. Reproduced with permissions [54], Copyright 2017, Wiley-VCH.

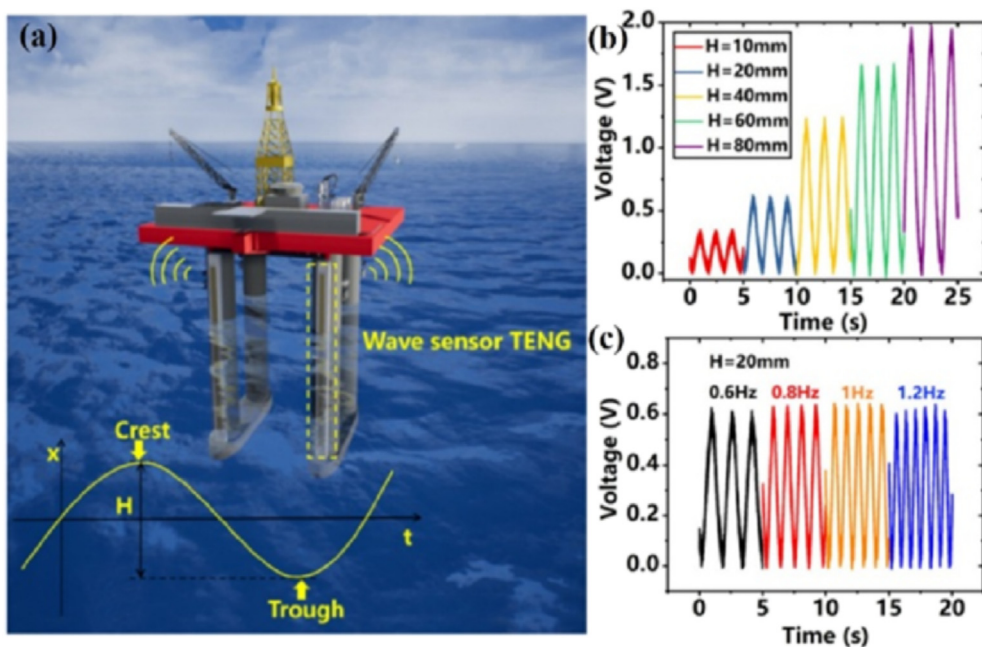


Fig. 15. (a) schematic of using a water-TENG device for self-powered wave sensing, (b) relationship between the measured output voltage and wave height, and (c) relationship between the measured output voltage and wave frequency. Reproduced with permissions [76], Copyright 2019, Elsevier.

right-side electrodes. The excess charges change the contact angle of the droplet on the actuation chip. Similarly, when the droplet slides to the right electrode, the same process happens, and a larger electric potential is generated between the two electrodes of the actuation chip, owing to the acceleration effect of the sliding droplet. A 46 V open-circuit voltage was achieved when an 80  $\mu$ L droplet slid down the sliding chip. Such an electric potential will induce a large contact angle

modification on the right side (Fig. 16d). The contact angle difference between the left and right sides of the droplet leads to an unbalanced pressure distribution in the droplet, and thus an actuation force is generated as follows:

$$F_d = \frac{1}{2} \pi r_0 \gamma_{LV} (\cos(\theta_R) - \cos(\theta_L)) \tag{6}$$

This droplet driving force could be derived from capillary force by

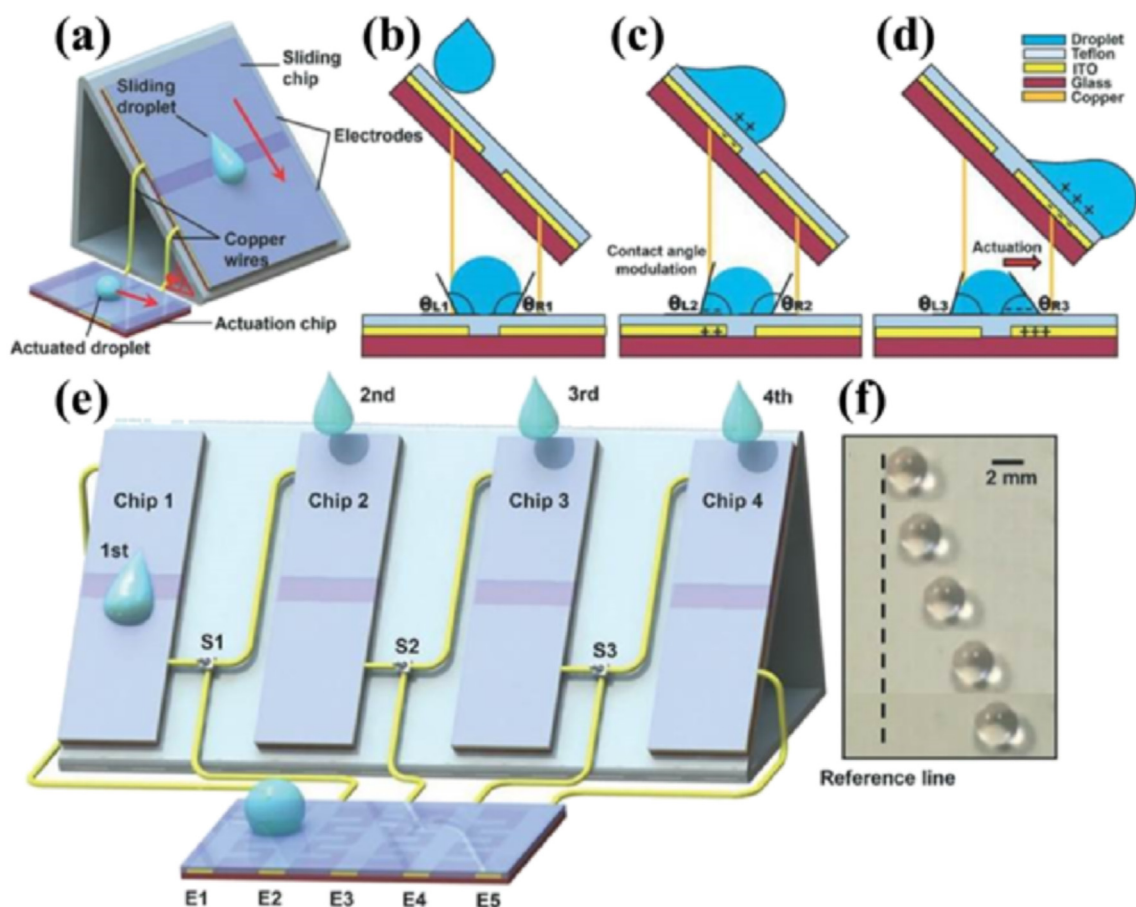


Fig. 16. Schematic of a droplet-based TENG device enabled self-powered droplet actuation system. Reproduced with permissions [29], Copyright 2018, Royal Society of Chemistry.

the Carre and Shanahan model, and more details on the derivation process can be found in Refs. [86,87]. In the above,  $r_0$  is the droplet base radius,  $\gamma_{LV}$  is the liquid-vapour surface tension, and  $\theta_R$  and  $\theta_L$  are the droplet right-side and left-side contact angles, respectively. When the actuation force is greater than the frictional force between the droplet and the surface, the droplet will be actuated without any external power supply. By properly designing the configuration of the electrodes and circuit as shown in Fig. 16e, a continuous droplet motion was achieved (Fig. 16f). The self-powered droplet motion would be helpful for replacing a bulky and costly power supply, and for building a portable microfluidic device for onsite applications [88].

## 5. Outlook of challenges and opportunities

In general, the water-TENG devices have been broadly demonstrated to harvest hydropower from renewable sources. The harvested energy could be stored in capacitors, or could be directly utilised in, e.g. self-powered sensors and actuators. Table 1 summarises the achievements of using water-TENG devices for energy harvesting and self-powered sensors/actuators.

It can be seen from Table 1 that water-TENG devices have been widely employed for harvesting hydropower. The output power density varies, based on the different working conditions and constituent materials. As an alternative method for harvesting hydropower (other than EMGs), the output power is still quite low in the current stage. This is mainly attributed to the small output current of the TENG devices. Nevertheless, the high output voltage is a very important feature of the TENG, and could even be used as a power source for electrospinning applications [93]. With the rapid development of Internet of things

(IoT), a large number of sensors are required for monitoring purposes [94]. Chemical batteries would involve inconvenience in discharge duration and replacement. TENG devices, with a self-powered feature, have great potential for sensor applications. Similarly, large numbers of sensors at a solid-liquid interface are required in the fields of multiphase flow, microfluidics, and so on [95,96]. Furthermore, the TENG technology has been developed in less than 10 years. With a further improvement of this technology, a large power output could be expected in the near future. Significant additional efforts should be conducted for improving the performance of water-TENG devices and broadening the applicability.

First, it is known that the tribo-charges on the hydrophobic layer are the basis for water-TENG energy harvesters. In the reported studies, the increase in the ion concentration is found to reduce the number of charges on the hydrophobic layer. A contact electrification model explains the formation of tribo-charges on the solid surface when interacting with water. However, the parameters affecting the polarity of the tribo-charges on the solid surface require more detailed investigation. A clear understanding regarding the formation of the tribo-charges could help further increase the output performance of the water-TENG energy harvesters, and enhance the sensitivity of the self-powered sensors.

Second, the water-TENG device involves interdisciplinary research fields, including knowledge on water dynamics and movement of triboelectric charges. The water dynamics cause significant effects on the output performance of water-TENG devices. Investigations on water dynamics have been widely conducted in the areas of heat transfer, fluid machinery, and so on. However, comprehensive studies on the water dynamics-induced interfacial charge transfer phenomena between water and water-TENG devices are rare. Some functional surfaces

**Table 1**

Summary of the achievements made in the water-solid based triboelectric nanogenerators (TENG) devices.

| Number | Source  | Working mode                             | Power density  | Application             | Reference |
|--------|---------|--|--|-------------------------|-----------|
| 1      | Droplet | Single-electrode                         | 9.1 $\mu\text{W}/\text{cm}^2$ (single droplet)<br>20 $\text{mW}/\text{cm}^2$ (shower mode) | Energy harvesting       | [24]      |
| 2      | Droplet | Sliding free-standing                    | 50 $\mu\text{W}/\text{cm}^2$ (single droplet)  | Energy harvesting       | [15]      |
| 3      | Droplet | Pressing-releasing                       | 0.3 $\mu\text{W}/\text{cm}^2$ (single droplet)   | Energy harvesting       | [34]      |
| 4      | Droplet | Single-electrode                         | 11.56 $\text{mW}/\text{cm}^2$ (shower mode)  | Energy harvesting       | [16]      |
| 5      | Droplet | Single-electrode                         | 9.01 $\mu\text{W}/\text{cm}^2$ (shower mode)   | Energy harvesting       | [89]      |
| 6      | Droplet | Single-electrode                         | 0.6 $\mu\text{W}/\text{cm}^2$ (shower mode)  | Energy harvesting       | [69]      |
| 7      | Droplet | Pressing-releasing                       | 13 $\mu\text{W}/\text{cm}^2$ (shower mode)   | Energy harvesting       | [57]      |
| 8      | Droplet | Single-electrode                         | 0.27 $\mu\text{W}/\text{cm}^2$ (single droplet)  | Hybrid solar cell       | [65]      |
| 9      | Droplet | Single-electrode                         | 17 $\mu\text{W}/\text{cm}^2$ (shower mode)   | Hybrid solar cell       | [66]      |
| 10     | Droplet | Single-electrode                         | 131 $\mu\text{W}/\text{cm}^2$ (shower mode)  | Ethanol sensor          | [37]      |
| 11     | Droplet | Sliding free-standing                    | 8 $\mu\text{W}/\text{cm}^2$ (single droplet)   | Smart umbrella          | [64]      |
| 12     | Wave    | Sliding free-standing                    | 6.67 $\mu\text{W}/\text{cm}^2$ (wave mode)   | Energy harvesting       | [18]      |
| 13     | Wave    | Sliding free-standing                    | 0.456 $\mu\text{W}/\text{cm}^2$ (wave mode)  | Distress signal emitter | [27]      |
| 14     | Wave    | Sliding free-standing                    | 14.7 $\mu\text{W}/\text{cm}^2$ (wave mode)   | Signal transmitter      | [51]      |
| 15     | Wave    | Sliding free-standing                    | 0.075 $\mu\text{W}/\text{cm}^2$ (wave mode)  | Visualised detector     | [74]      |
| 16     | Wave    | Sliding free-standing enclosed structure | 200 $\mu\text{W}/\text{cm}^2$  | Energy harvesting       | [32]      |
| 17     | Wave    | Sliding free-standing enclosed structure | 1.05 $\mu\text{W}/\text{cm}^3$   | Energy harvesting       | [90]      |
| 18     | Wave    | Sliding free-standing enclosed structure | 27.12 $\mu\text{W}/\text{cm}^2$  | Energy harvesting       | [91]      |
| 19     | Wave    | Contact-separation enclosed structure    | 260 $\mu\text{W}/\text{cm}^2$  | Energy harvesting       | [92]      |
| 20     | Stream  | Single-electrode                         | 59 $\mu\text{W}/\text{cm}^2$ (stream mode)   | Energy harvesting       | [17]      |

with special water transport phenomena, including wettability gradient surfaces and hydrophobic/hydrophilic heterogeneous surfaces, could open up new opportunities for water-solid interfacial charge transfer phenomena and hydropower harvesting.

Third, applications of water-TENG devices for self-powered sensors have been reported for ocean waves and ethanol concentrations. However, the current demonstrations of using water-TENG devices as actuators are inadequate, and portable actuators without external power sources are strongly desired in robotics, digital microfluidics, micro-optics, and so on.

Fourth, most current water-TENG devices are developed at a lab scale, which is still far from the industrial requirements. Special attention should be paid to solving the engineering problems, including load matching, system integration, and control systems. Moreover, the cost and payback period are also very important factors when discussing real applications. The solid-solid based TENG devices are estimated with a very short payback period of approximately 0.05–0.3 years, depending on the efficiency and lifetime of the devices [97]. The levelised cost of electricity produced with solid-solid TENGs ranges from 2 to 13 US cents/kWh, which is much lower than that of traditional energy sources (7.04–11.9 US cents/kWh). However, the cost and payback period problems have not been addressed in water-TENG devices.

## Acknowledgements

Research was supported by the National Natural Science Foundation of China (Grant No. 51906031, 51879022), the National Key Research and Development Program of China (Grant No. 2016YFA0202704), the ‘Thousands Talents’ program for pioneer researcher and his innovation team in China.

## References

- Ö Wikander. Sources of energy and exploitation of power. The Oxford handbook of engineering and technology in the classical world. 2008.
- Jawahar C, Michael PA. A review on turbines for micro hydro power plant. *Renew Sustain Energy Rev* 2017;72:882–7.
- Zervos A, Lins C, Renewables. 2016 global status report. Council of the Federation; 2016.
- Chen Z, Chen D, Xu K, Zhao Y, Wei T, Chen J, et al. Acoustic Doppler current profiler surveys along the Yangtze River. *Geomorphology* 2007;85:155–65.
- Zarfi C, Lumsdon AE, Berlekamp J, Tydecks L, Tockner K. A global boom in hydropower dam construction. *Aquat Sci* 2015;77:161–70.
- Wang X, Song J, Liu J, Wang ZL. Direct-current nanogenerator driven by ultrasonic waves. *Science* 2007;316:102–5.
- Chang C, Tran VH, Wang J, Fuh Y-K, Lin L. Direct-write piezoelectric polymeric nanogenerator with high energy conversion efficiency. *Nano Lett* 2010;10:726–31.
- Zhang C, Tang W, Han C, Fan F, Wang ZL. Theoretical comparison, equivalent transformation, and conjunction operations of electromagnetic induction generator and triboelectric nanogenerator for harvesting mechanical energy. *Adv Mater* 2014;26:3580–91.
- Bai P, Zhu G, Lin Z-H, Jing Q, Chen J, Zhang G, et al. Integrated multilayered triboelectric nanogenerator for harvesting biomechanical energy from human motions. *ACS Nano* 2013;7:3713–9.
- Wang ZL. On Maxwell's displacement current for energy and sensors: the origin of nanogenerators. *Mater Today* 2017;20.
- Yoon H-J, Ryu H, Kim S-W. Sustainable powering triboelectric nanogenerators: approaches and the path towards efficient use. *Nano Energy* 2018;51:270–85.
- Fan F-R, Tian Z-Q, Wang ZL. Flexible triboelectric generator. *Nano Energy* 2012;1:328–34.
- Zhu G, Zhou YS, Bai P, Meng XS, Jing Q, Chen J, et al. A shape-adaptive thin-film-based approach for 50% high-efficiency energy generation through micro-grating sliding electrification. *Adv Mater* 2014;26:3788–96.
- Xie Y, Wang S, Niu S, Lin L, Jing Q, Yang J, et al. Grating-structured freestanding triboelectric-layer nanogenerator for harvesting mechanical energy at 85% total conversion efficiency. *Adv Mater* 2014;26:6599–607.
- Kwon SH, Park J, Kim WK, Yang YJ, Lee E, Han CJ, et al. An effective energy harvesting method from a natural water motion active transducer. *Energy Environ Sci* 2014;7:3279–83.
- Liang Q, Yan X, Gu Y, Zhang K, Liang M, Lu S, et al. Highly transparent triboelectric nanogenerator for harvesting water-related energy reinforced by antireflection coating. *Sci Rep* 2015;5:9080.
- Cheng G, Lin ZH, Du ZL, Wang ZL. Simultaneously harvesting electrostatic and mechanical energies from flowing water by a hybridized triboelectric nanogenerator. *ACS Nano* 2014;8:1932–9.
- Zhu G, Su Y, Peng B, Chen J, Jing Q, Yang W, et al. Harvesting water wave energy by asymmetric screening of electrostatic charges on a nanostructured hydrophobic thin-film surface. *ACS Nano* 2014;8:6031.
- Tang W, Chen BD, Wang ZL. Recent progress in power generation from water/liquid droplet interaction with solid surfaces. *Adv Funct Mater* 2019;1901069.
- Wang ZL, Wang AC. On the origin of contact-electrification. *Mater Today* 2019.
- Xu C, Wang AC, Zou H, Zhang B, Zhang C, Zi Y, et al. Raising the working temperature of a triboelectric nanogenerator by quenching down electron thermionic emission in contact-electrification. *Adv Mater* 2018;30:e1803968.
- JCM III FRS. On physical lines of force. *Philos Mag* 1971;23:13.
- Wang ZL, Jiang T, Xu L. Toward the blue energy dream by triboelectric nanogenerator networks. *Nano Energy* 2017;39:9–23.
- Lin ZH, Cheng G, Lee S, Pradel KC, Wang ZL. Harvesting water drop energy by a sequential contact-electrification and electrostatic-induction process. *Adv Mater* 2014;26:4690–6.
- Wang J, Wu Z, Pan L, Gao R, Zhang B, Yang L, et al. Direct-current rotary-tubular triboelectric nanogenerators based on liquid-dielectrics contact for sustainable energy harvesting and chemical composition analysis. *ACS Nano* 2019;13:2587–98.
- Lin ZH, Gang C, Li X, Yang PK, Wen X, Zhong LW. A multi-layered interdigitated-electrodes-based triboelectric nanogenerator for harvesting hydropower. *Nano Energy* 2015;15:256–65.
- Su Y, Wen X, Zhu G, Yang J, Chen J, Bai P, et al. Hybrid triboelectric nanogenerator for harvesting water wave energy and as a self-powered distress signal emitter. *Nano Energy* 2014;9:186–95.
- Helseth LE, Guo XD. Hydrophobic polymer covered by a grating electrode for converting the mechanical energy of water droplets into electrical energy. *Smart Mater Struct* 2016;25:045007.
- Chen G, Liu X, Li S, Dong M, Jiang D. A droplet energy harvesting and actuation system for self-powered digital microfluidics. *Lab Chip* 2018;18:1026.

- [30] Xi Y, Wang J, Zi Y, Li X, Han C, Cao X, et al. High efficient harvesting of underwater ultrasonic wave energy by triboelectric nanogenerator. *Nano Energy* 2017;38:101–8.
- [31] Feng L, Liu G, Guo H, Tang Q, Pu X, Chen J, et al. Hybridized nanogenerator based on honeycomb-like three electrodes for efficient ocean wave energy harvesting. *Nano Energy* 2018;47:217–23.
- [32] Wang X, Niu S, Yin Y, Yi F, You Z, Wang ZL. Triboelectric nanogenerator based on fully enclosed spherical structure for harvesting low-frequency water wave energy. *Adv Energy Mater* 2015;5:1501467.
- [33] Nguyen V, Zhu R, Yang R. Environmental effects on nanogenerators. *Nano Energy* 2015;14:49–61.
- [34] Moon JK, Jeong J, Lee D, Pak HK. Electrical power generation by mechanically modulating electrical double layers. *Nat Commun* 2013;4:1487.
- [35] Krupenkin T, Taylor JA. Reverse electrowetting as a new approach to high-power energy harvesting. *Nat Commun* 2011;2:448.
- [36] Helseth LE, Guo XD. Contact electrification and energy harvesting using periodically contacted and squeezed water droplets. *Langmuir the ACS Journal of Surfaces & Colloids* 2015;31:3269–76.
- [37] Lin Z-H, Cheng G, Wu W, Pradel KC, Wang ZL. Dual-mode triboelectric nanogenerator for harvesting water energy and as a self-powered ethanol nanosensor. *ACS Nano* 2014;8:6440–8.
- [38] Yang Y, Park J, Kwon SH, Kim YS. Fluidic active transducer for electricity generation. *Sci Rep* 2015;5:15695.
- [39] Bardeen J. Electrical conductivity of metals. *J Appl Phys* 1940;11:88–111.
- [40] Liu XM, Huang ZD, Oh SW, Zhang B, Ma PC, Yuen MMF, et al. Carbon nanotube (CNT)-based composites as electrode material for rechargeable Li-ion batteries: a review. *Compos Sci Technol* 2012;72:121–44.
- [41] Wang X, Linjie Zhi A, Müllen K. Transparent, conductive graphene electrodes for dye-sensitized solar cells. *Nano Lett* 2008;8:323.
- [42] Xin Z, Hui T, Zhu M, Kai T, Wang JJ, Kang F, et al. Carbon nanosheets as the electrode material in supercapacitors. *J Power Sources* 2009;194:1208–12.
- [43] Park J, Yang Y, Kwon SH, Kim YS. Influences of surface and ionic properties on electricity generation of an active transducer driven by water motion. *J Phys Chem Lett* 2015;6:150204151146006.
- [44] Yun BK, Kim HS, Ko YJ, Murillo G, Jung JH. Interdigital electrode based triboelectric nanogenerator for effective energy harvesting from water. *Nano Energy* 2017;36:233–40.
- [45] Choi D, Lee H, Im DJ, Kang IS, Lim G, Dong SK, et al. Spontaneous electrical charging of droplets by conventional pipetting. *Sci Rep* 2013;3:2037.
- [46] Wang S, Xie Y, Niu S, Lin L, Liu C, Zhou YS, et al. Maximum surface charge density for triboelectric nanogenerators achieved by ionized-air injection: methodology and theoretical understanding. *Adv Mater* 2014;26:6720–8.
- [47] Liu W, Wang Z, Wang G, Liu G, Chen J, Pu X, et al. Integrated charge excitation triboelectric nanogenerator. *Nat Commun* 2019;10:1426.
- [48] Yeong YH, Burton J, Loth E, Bayer IS. Drop impact and rebound dynamics on an inclined superhydrophobic surface. *Langmuir : the ACS journal of surfaces and colloids* 2014;30:12027–38.
- [49] Shen C, Yu C, Chen Y. Spreading dynamics of droplet on an inclined surface. *Theor Comput Fluid Dyn* 2015;30:237–52.
- [50] Choi D, Kim DW, Yoo D, Cha KJ, La M, Dong SK. Spontaneous occurrence of liquid-solid contact electrification in nature: toward a robust triboelectric nanogenerator inspired by the natural lotus leaf. *Nano Energy* 2017;36:250–9.
- [51] Zhao XJ, Kuang SY, Wang ZL, Zhu G. Highly adaptive solid-liquid interfacing triboelectric nanogenerator for harvesting diverse water wave energy. *ACS Nano* 2018;12:4280.
- [52] Jiang D, Guo F, Xu M, Cai J, Cong S, Jia M, et al. Conformal fluorine coated carbon paper for an energy harvesting water wheel. *Nano Energy* 2019;58:842–51.
- [53] Pan L, Wang J, Wang P, Gao R, Wang Y-C, Zhang X, et al. Liquid-FEP-based U-tube triboelectric nanogenerator for harvesting water-wave energy. *Nano Res* 2018;11:4062–73.
- [54] Chen BD, Tang W, He C, Jiang T, Xu L, Zhu LP, et al. Ultrafine capillary-tube triboelectric nanogenerator as active sensor for microliquid biological and chemical sensing. *Adv Mater Tech* 2018;3:1700229.
- [55] Qiao Y, Feng J, Liu X, Wang W, Zhang P, Zhu L. Surface water pH variations and trends in China from 2004 to 2014. *Environ Monit Assess* 2016;188:443.
- [56] Wu Y, Su Y, Bai J, Zhu G, Zhang X, Li Z, et al. A self-powered triboelectric nanosensor for PH detection. *J Nanom* 2016;2016(2016–2–21). 2016:1.
- [57] Lin ZH, Cheng G, Lin L, Lee S, Wang ZL. Water-solid surface contact electrification and its use for harvesting liquid-wave energy. *Angew Chem Int Ed* 2013;52:12545–9.
- [58] Owen BB, Miller RC, Milner CE, Cogan HL. The dielectric constant of water as a function of temperature and pressure 1.2. *J Phys Chem* 1961;65:2065–70.
- [59] Jin Z, Sui D, Yang Z. The impact, freezing, and melting processes of a water droplet on an inclined cold surface. *Int J Heat Mass Transf* 2015;90:439–53.
- [60] Yarin AL. ... Drop impact dynamics: splashing, spreading, receding, bouncing. *Annu Rev Fluid Mech* 2006;38:159–92.
- [61] Leclear S, Leclear J, Abhijeet, Park KC, Choi W. Drop impact on inclined superhydrophobic surfaces. *J Colloid Interface Sci* 2016;461:114–21.
- [62] Liu C, Jing S, Jing L, Xiang C, Che L, Wang Z, et al. Long-range spontaneous droplet self-propulsion on wettability gradient surfaces. *Sci Rep* 2017;7:7552.
- [63] Yang X, Chan S, Wang L, Daoud WA. Water tank triboelectric nanogenerator for efficient harvesting of water wave energy over a broad frequency range. *Nano Energy* 2018;44:388–98.
- [64] Kwon SH, Kim WK, Park J, Yang Y, Yoo B, Han CJ, et al. Fabric active transducer stimulated by water motion for self-powered wearable device. *ACS Appl Mater Interfaces* 2016;8:24579–84.
- [65] Jeon SB, Kim D, Yoon GW, Yoon JB, Choi YK. Self-cleaning hybrid energy harvester to generate power from raindrop and sunlight. *Nano Energy* 2015;12:636–45.
- [66] Zheng L, Lin ZH, Cheng G, Wu W, Wen X, Lee S, et al. Silicon-based hybrid cell for harvesting solar energy and raindrop electrostatic energy. *Nano Energy* 2014;9:291–300.
- [67] Pu X, Song W, Liu M, Sun C, Du C, Jiang C, et al. Wearable power-textiles by integrating fabric triboelectric nanogenerators and fiber-shaped dye-sensitized solar cells. *Adv Energy Mater* 2016;6:1601048.
- [68] Cho Y, Lee S, Hong J, Pak S, Bo H, Lee YW, et al. Sustainable hybrid energy harvester based on air stable quantum dot solar cells and triboelectric nanogenerator. *J Mater Chem A* 2018;6.
- [69] Zheng L, Cheng G, Chen J, Lin L, Wang J, Liu Y, et al. A hybridized power panel to simultaneously generate electricity from sunlight, raindrops, and wind around the clock. *Adv Energy Mater* 2015;5:1501152.
- [70] Kim T, Chung J, Kim DY, Moon JH, Lee S, Cho M, et al. Design and optimization of rotating triboelectric nanogenerator by water electrification and inertia. *Nano Energy* 2016;27:340–51.
- [71] Park HY, Kim HK, Hwang YH, Shin DM. Water-through triboelectric nanogenerator based on Ti-mesh for harvesting liquid flow. *J Korean Phys Soc* 2018;72:499–503.
- [72] Zhong LW. Triboelectric nanogenerators as new energy technology for self-powered systems and as active mechanical and chemical sensors. *ACS Nano* 2013;7:9533.
- [73] Zhang X, Zheng Y, Wang D, Feng Z. Solid-liquid triboelectrification in smart U-tube for multifunctional sensors. *Nano Energy* 2017;40.
- [74] Han M, Yu B, Qiu G, Chen H, Su Z, Shi M, et al. Electrification based devices with encapsulated liquid for energy harvesting, multifunctional sensing, and self-powered visualized detection. *J Mater Chem A* 2015;3:7382–8.
- [75] Zhang H, Yang Y, Su Y, Chen J, Hu C, Wu Z, et al. Triboelectric nanogenerator as self-powered active sensors for detecting liquid/gaseous water/ethanol. *Nano Energy* 2013;2:693–701.
- [76] Xu M, Wang S, Zhang SL, Ding W, Kien PT, Wang C, et al. A highly-sensitive wave sensor based on liquid-solid interfacing triboelectric nanogenerator for smart marine equipment. *Nano Energy* 2019;57:574–80.
- [77] Chen J, Guo H, Zheng J, Huang Y, Liu G, Hu C, et al. Self-powered triboelectric micro liquid/gas flow sensor for microfluidics. *ACS Nano* 2016;10:8104–12.
- [78] Zhang X, Yu M, Ma Z, Ouyang H, Zou Y, Zhang SL, et al. Self-powered distributed water level sensors based on liquid-solid triboelectric nanogenerators for ship draft detecting. *Adv Funct Mater* 2019:1900327.
- [79] Daniela R, Tolley MT. Design, fabrication and control of soft robots. *Nature* 2015;521:467–75.
- [80] Tavakoli M, Rui PR, Lourenço J, Tong L, Majidi C. Soft bionics hands with a sense of touch through an electronic skin. *Soft robotics: trends, applications and challenges*. Springer; 2017.
- [81] Zhang S, Yu Z, Li P, Li B, Isikgor FH, Du D, et al. Poly(3,4-ethylenedioxythiophene):polystyrene sulfonate films with low conductivity and low acidity through a treatment of their solutions with probe ultrasonication and their application as hole transport layer in polymer solar cells and perovskite solar cells. *Org Electron* 2016;32:149–56.
- [82] Khaldi A, Maziz A, Alici G, Spinks GM, Jager EWH. Bottom-up microfabrication process for individually controlled conjugated polymer actuators. *Sens Actuators B Chem* 2016;230:818–24.
- [83] Chen X, Jiang T, Wang ZL. Modeling a dielectric elastomer as driven by triboelectric nanogenerator. *Appl Phys Lett* 2017;110:033505.
- [84] Zhang C, Tang W, Pang Y, Han C, Wang ZL. Active micro-actuators for optical modulation based on a planar sliding triboelectric nanogenerator. *Adv Mater* 2015;27:719–26.
- [85] Li X, Liu M, Huang B, Liu H, Hu W, Shao LH, et al. Nanoporous-gold-based hybrid cantilevered actuator dealloyed and driven by A modified rotary triboelectric nanogenerator. *Sci Rep* 2016;6:24092.
- [86] Abdelgawad M, Freire SLS, Yang H, Wheeler AR. All-terrain droplet actuation. *Lab Chip* 2008;8:672.
- [87] Carre A, Shanahan MER. Drop motion on an inclined plane and evaluation of hydrophobia treatments to glass. *J Adhes* 2006;49:177–85.
- [88] Jiang D, Lee S, Bae SW, Park SY. Smartphone integrated optoelectrowetting (SiOEW) for on-chip sample processing and microscopic detection of water quality. *Lab Chip* 2018(18):532–9. 10.1039.C7LC01095H.
- [89] Sun Y, Huang X, Soh S. Using the gravitational energy of water to generate power by separation of charge at interfaces. *Chem Sci* 2015;6:3347–53.
- [90] Wang X, Wen Z, Guo H, Wu C, He X, Lin L, et al. Fully packaged blue energy harvester by hybridizing a rolling triboelectric nanogenerator and an electromagnetic generator. *ACS Nano* 2016;10:11369–76.
- [91] Wen Z, Guo H, Zi Y, Yeh MH, Wang X, Deng J, et al. Harvesting broad frequency band blue energy by a triboelectric-electromagnetic hybrid nanogenerator. *ACS Nano* 2016;10:6526–34.
- [92] Chen J, Yang J, Li Z, Fan X, Zi Y, Jing Q, et al. Networks of triboelectric nanogenerators for harvesting water wave energy: a potential approach toward blue energy. *ACS Nano* 2015;9:3324–31.
- [93] Li C, Yin Y, Wang B, Zhou T, Wang J, Luo J, et al. Self-powered electrospinning system driven by a triboelectric nanogenerator. *ACS Nano* 2017;11:10439–45.
- [94] Wang S, Lin L, Wang ZL. Triboelectric nanogenerators as self-powered active sensors. *Nano Energy* 2015;11:436–62.
- [95] Young YL, Harwood CM, Ward JC. Sensing and control of flexible hydrodynamic lifting bodies in multiphase flows. *Sensors and smart structures technologies for civil, mechanical, and aerospace systems* 2018. *Int Soc Opt Phot* 2018:105981N.
- [96] Altintas Z, Akgun M, Kokturk G, Uludag Y. A fully automated microfluidic-based electrochemical sensor for real-time bacteria detection. *Biosens Bioelectron* 2018;100:541–8.
- [97] Ahmed A, Hassan I, Ibn-Mohammed T, Mostafa H, Reaney IM, Koh LSC, et al. Environmental life cycle assessment and techno-economic analysis of triboelectric nanogenerators. *Energy Environ Sci* 2017;10:653–71.